

AD-A065 464

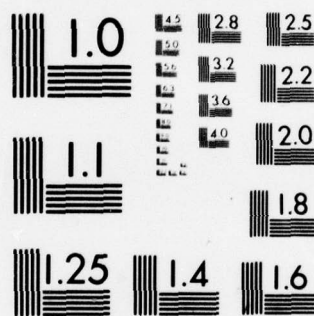
DAEDALEAN ASSOCIATES INC WOODBINE MD  
THE RESEARCH AND DEVELOPMENT OF A CAVITATING WATER JET CLEANING--ETC(U)  
DEC 78 S C HOWARD, D R KOOGLE, A A HOCHREIN N00014-77-C-0367  
DAI-SH-7759-002-TR NL

UNCLASSIFIED

| OF |

AD  
A065 464





MICROCOPY RESOLUTION TEST CHART  
NATIONAL BUREAU OF STANDARDS-1963-A

**LEVEL**

*III*  
*A065-463*

**(3)**

**DAEDALEAN ASSOCIATES, INC.**

ENGINEERING, DESIGN AND ANALYSIS SERVICES

**AD A065464**



**DDC FILE COPY**

**DDC**  
**RECEIVED**  
MAR 2 1979  
**RECEIVED**  
**D**

**DISTRIBUTION STATEMENT A**

Approved for public release;  
Distribution Unlimited



**SPRINGLAKE RESEARCH CENTER**  
**15110 FREDERICK ROAD**  
**WOODBINE, MARYLAND 21797**

ORIGINAL CONTAINS COLOR PLATES: ALL DDC  
REPRODUCTIONS WILL BE IN BLACK AND WHITE.

**79 02 26 229**

DAEDALEAN ASSOCIATES, Incorporated

LEVEL III

3

9 TECHNICAL REPORT

AD A0 65464

DDC FILE COPY

6 THE RESEARCH AND DEVELOPMENT OF  
A CAVITATING WATER JET CLEANING  
SYSTEM FOR REMOVING MARINE GROWTH  
AND FOULING FROM OFFSHORE PLATFORM  
STRUCTURES: FEASIBILITY EVALUATION

Submitted to

SHIP TECHNOLOGY PROGRAM  
CODE 221

OFFICE OF NAVAL RESEARCH  
DEPARTMENT OF THE NAVY  
ARLINGTON, VIRGINIA 22217

12 60p.

by

ACCESSION FOR	
NTIS	White Section <input checked="" type="checkbox"/>
DDC	Ref Section <input type="checkbox"/>
UNANNOUNCED	<input type="checkbox"/>
JUSTIFICATION	
Per Hq. (FL-88/RN-0289)	
BY on file	
DISTRIBUTION/AVAILABILITY CODES	
DIRL	AVAIL. and/or SPECIAL
A	

10 Stephen C./Howard,

Dwight R./Koogler

A. A./Hochrein, Jr

DDC  
RECEIVED  
MAR 2 1979  
D

The views and conclusions contained in this document are those of the authors and should not be interpreted as necessarily representing the official policies, either expressed or implied of the Department of Defense or the U. S. Government.

Prepared for the Office of Naval Research, Ship Technology Program under Contract No. N00014-77-C-0367

14 DAI SH-7759-002-TR

DISTRIBUTION STATEMENT A

Approved for public release;  
Distribution Unlimited

11 Dec 1978

ORIGINAL CONTAINS COLOR PLATES: ALL DDC  
REPRODUCTIONS WILL BE IN BLACK AND WHITE.

79 02 26 229  
390 758



ACKNOWLEDGMENTS

This report is submitted in partial fulfillment of Office of Naval Research contract number N00014-77-C-0367. The technical program was developed under the sponsorship of LCDR Hal Martin, Code 211, Office of Naval Research. His technical advice was instrumental in obtaining the outcome of this investigation.

Messrs. William Boyd and Tom Stansfield of DAEDALEAN ASSOCIATES, Inc. provided the technical assistance necessary for the fulfillment of the engineering requirements of this program.

TABLE OF CONTENTS

	<u>Page</u>
ACKNOWLEDGMENTS . . . . .	i
NOTATION . . . . .	iv
LIST OF FIGURES . . . . .	v
1.0 INTRODUCTION . . . . .	1
1.1 Background . . . . .	2
1.2 Program Summary . . . . .	3
2.0 EXPERIMENTAL FACILITY AND TECHNIQUES . . . . .	5
2.1 High Pressure Water Flow and Delivery Subsystem to the Cleaning Nozzles . . . . .	5
2.2 Control and Instrumentation Subsystem . . . . .	6
2.3 Nozzle Performance and Fouling Removal Evaluation Subsystem . . . . .	7
3.0 EXPERIMENTAL RESULTS AND DISCUSSION . . . . .	9
3.1 Program Approach . . . . .	9
3.2 Initial Nozzle Configurations . . . . .	10
3.3 Operating Parameters . . . . .	10
3.3.1 Loss Coefficient . . . . .	10
3.3.2 Intensity of Erosion . . . . .	12
3.3.3 Cleaning Rate Data . . . . .	13
3.3.3.1 Nozzle Diameter Deter- mination for Cleaning Rate Data . . . . .	14
3.3.3.2 Threshold Intensity of Erosion for Barnacles and Steel Substrate Material . . . . .	16

TABLE OF CONTENTS (CONT.)

	<u>Page</u>
3.3.3.3 Cleaning Rate Data Tests . . .	17
3.4 Horsepower Requirements . . . . .	17
4.0 CONCLUSIONS AND RECOMMENDATIONS . . . . .	18
APPENDIX	

NOTATION

- $I_e$  - intensity of erosion
- $P_i$  - the impact pressure arising from bubble collapse
- $P_o$  - free stream pressure
- $P_v$  - vapor pressure of liquid
- $R$  - the size of the bubble or jet
- $\Delta t$  - time of erosion
- $V_o$  - velocity of the free stream
- $\Delta y$  - drilling depth of erosion
- area of cleaning
- $\rho$  - density of liquid
- $\sigma$  - cavitation number
- $E$  - energy absorbed by the material removed
- $\Delta V$  - volume of material removed
- $S$  - scale strength
- $n$  - number of impacts per unit time
- $C_v$  - coefficient of velocity



LIST OF FIGURES

- FIGURE 1 - CONCAVER<sup>TM</sup> TECHNIQUE FOR CLEANING OFFSHORE PLATFORM STRUCTURES
- FIGURE 2 - HIGH PRESSURE TRIPLEX PLUNGER PUMP
- FIGURE 3 - DAI CLEANING RATE MECHANISM
- FIGURE 4 - FOULED PLATE BEING CLEANED UTILIZING CONCAVER TECHNIQUE
- FIGURE 5 - LOSS COEFFICIENT AS A FUNCTION OF NOZZLE PRESSURE FOR A SINGLE ORIFICE CONICAL NOZZLE
- FIGURE 6 - LOSS COEFFICIENT AS A FUNCTION OF NOZZLE PRESSURE FOR THREE CONFIGURATIONS OF THE 0.042 IN. DIAMETER NOZZLE
- FIGURE 7 - LOSS COEFFICIENT AS A FUNCTION OF NOZZLE PRESSURE FOR THREE CONFIGURATIONS OF THE 0.047 IN. DIAMETER NOZZLE
- FIGURE 8 - INTENSITY OF EROSION AS A FUNCTION OF NOZZLE DISTANCE FOR A 0.042 IN. DIAMETER NOZZLE WITH NO SWIRL AT THREE PRESSURES
- FIGURE 9 - INTENSITY OF EROSION AS A FUNCTION OF NOZZLE DISTANCE FOR A 0.042 IN. DIAMETER NOZZLE WITH A NUMBER 46 SWIRL INSERT AT THREE PRESSURES
- FIGURE 10 - INTENSITY OF EROSION AS A FUNCTION OF NOZZLE DISTANCE FOR A 0.042 IN. DIAMETER NOZZLE WITH A NUMBER 45 SWIRL INSERT AT THREE PRESSURES
- FIGURE 11 - INTENSITY OF EROSION AS A FUNCTION OF NOZZLE DISTANCE FOR A 0.047 IN. DIAMETER NOZZLE WITH NO SWIRL INSERT AT THREE PRESSURES
- FIGURE 12 - INTENSITY OF EROSION AS A FUNCTION OF NOZZLE DISTANCE FOR A 0.047 IN. DIAMETER NOZZLE WITH A NUMBER 46 SWIRL INSERT AT THREE PRESSURES
- FIGURE 13 - INTENSITY OF EROSION AS A FUNCTION OF NOZZLE DISTANCE FOR A 0.047 IN. DIAMETER NOZZLE WITH A NUMBER 45 SWIRL INSERT AT THREE PRESSURES



- FIGURE 14 - LOSS COEFFICIENT AS A FUNCTION OF NOZZLE PRESSURE FOR THREE CONFIGURATIONS OF THE 0.023 INCH DIAMETER NOZZLE
- FIGURE 15 - LOSS COEFFICIENT AS A FUNCTION OF NOZZLE PRESSURE FOR THREE CONFIGURATIONS OF THE 0.031 INCH DIAMETER NOZZLE
- FIGURE 16 - INTENSITY OF EROSION AS A FUNCTION OF NOZZLE DISTANCE FOR THREE CONFIGURATIONS OF THE 0.023 INCH DIAMETER NOZZLE, OPERATING PRESSURE = 14,000 PSI
- FIGURE 17 - INTENSITY OF EROSION AS A FUNCTION OF NOZZLE DISTANCE FOR THREE CONFIGURATIONS OF THE 0.031 INCH DIAMETER NOZZLE, OPERATING PRESSURE = 14,000 PSI
- FIGURE 18 - THRESHOLD INTENSITY FOR BARNACLE REMOVAL FROM PLATFORM STRUCTURE
- FIGURE 19 - MEASURED POWER OUTPUT AND CLEANING RATE AS A FUNCTION OF NOZZLE DIAMETER USING SINGLE ORIFICE NOZZLES WITH AND WITHOUT SWIRLS
- FIGURE 20 - TEST PANEL FROM WHICH THE EPOXY VINYL COATING AND FOULING WAS REMOVED FROM ONE HALF THE AREA AT A CLEANING RATE OF 16 FT<sup>2</sup>/HR

#### APPENDIX A

- FIGURE A-1 - PRINCIPLE OF CONTROLLED CAVITATION CLEANING TECHNIQUE AS APPLIED TO REMOVAL OF MARINE GROWTH AND FOULING FROM OFFSHORE PLATFORM STRUCTURAL MEMBER
- FIGURE A-2 - PHOTOGRAPHIC REPRESENTATION OF THE CAVITATING ENVELOPE DURING WHICH TIME THE BUBBLES FORM A NUCLEI, GROW TO CRITICAL SIZE AND COLLAPSE IN THE CONTINUOUS CAVITATION PROCESS
- FIGURE A-3 - MASTER CHART FOR CAVITATION EROSION
- FIGURE A-4 - EROSION INTENSITY ESTIMATOR

THE RESEARCH AND DEVELOPMENT OF  
A CAVITATING WATER JET CLEANING  
SYSTEM FOR REMOVING MARINE GROWTH  
AND FOULING FROM OFFSHORE PLATFORM  
STRUCTURES: FEASIBILITY EVALUATION

1.0 INTRODUCTION

Inspection of offshore structures for safety and reliability is an important operating consideration in the design of platforms and towers. As these structures approach design life and are subject to in-service utilization by the offshore industry, it is imperative that proper inspection procedures be employed. The various inspection procedures presently being used in the field require an efficient method for removing the marine growth and the associated protective coating from the offshore structures before these nondestructive evaluation techniques can be effectively used for crack detection and platform deterioration. Furthermore, current corrosion mechanisms including crevice corrosion and pitting corrosion are initiated and aided by the attachment of marine organisms. Periodic removal of marine growth from offshore platform structures would reduce the corrosion rates and increase the service life of these structures thereby enhancing the safety and reliability of in-service operations.

The complex nature of the structural sections, including "I" sections; angles; channels; joints; weldments; etc., makes it difficult and time consuming for divers to use conventional

brushes and hydroblasting techniques for removing marine growth. Some of the organisms produce strong calcareous cements which cannot currently be removed even by wire brush techniques. These operational difficulties, combined with the dynamic and hydrostatic forces of the ocean environment, make it difficult to remove offshore structure marine growth as periodically required so that safety inspections can be performed at regular intervals. Because of these reasons, there is a requirement to develop an effective, simple, and economic method to remove the marine growth and associated protective coatings from offshore structures.

### 1.1 Background

With these objectives in mind, DAEDALEAN ASSOCIATES, Inc. (DAI), under contract to the Office of Naval Research (ONR), has conducted an initial research and development program to assess the technical feasibility of utilizing cavitation for removing marine growth and the protective coating from offshore platform structures. Figure 1 shows a conceptual rendition of a diver-operated offshore platform cleaning system utilizing the CONCAVER<sup>TM</sup> (controlled cavitation erosion) technique. With this technique, water is pumped under pressure through a properly designed nozzle and cleaning system. The high speed jet emerging from the nozzle produces cavitation bubbles which collapse on the surface. As the high pressure jet emerges from the cavitating nozzle, the large number of cavitation bubbles follow the jet stream. By carefully controlling the intensity of collapse of



these cavitation bubbles, the marine growth and protective coating can be selectively and rapidly removed without damaging the substrate material.

A discussion of the cavitation phenomenon is presented in Appendix A.

### 1.2 Program Summary

The technical feasibility of using the cavitating water jet technique for removing marine growth and protective coatings from steel substrate material has been demonstrated under laboratory conditions in the initial phase of the program. The test results for this phase indicate that the CONCAVER<sup>TM</sup> technique can remove the fouling and coating from test panels that had been submerged in the Atlantic Ocean for up to 36 months. Test panels coated with epoxy vinyl were cleaned to bare metal. Cleaning rates of approximately 16 <sup>sq ft</sup> ft<sup>2</sup>/hr. for removal of the fouling and coating to bare metal were obtained with this technique. The horsepower requirement corresponding to this rate of removal was approximately 22 hp.

The results of the initial technical feasibility evaluation defined various design parameters such as removal rates, area covered, nozzle size, loss coefficient, operating pressure, intensity of erosion, jet velocity, and horsepower requirements. Specific nozzle designs were evaluated with the intensity of erosion established as a function of nozzle distance. A threshold intensity of erosion design chart has been characterized

for barnacle removal. This chart identifies the margin of safety between the peak intensity of erosion and the threshold intensity for the steel substrate material. For the optimum operating conditions, cleaning rates were established for the removal of the marine growth and epoxy vinyl coating.



## 2.0 EXPERIMENTAL FACILITY AND TECHNIQUES

The requirements for the design and assembly of the laboratory apparatus along with the establishment of the test facility have been accomplished. The test facility consists of several subsystems for producing cavitating water jets and evaluating their effectiveness as a technique for fouling removal. These subsystems include: 1) high pressure water flow subsystem; 2) monitoring and control subsystem; and 3) nozzle performance and fouling removal evaluation subsystem.

### 2.1 High Pressure Water Flow and Delivery Subsystem to the Cleaning Nozzles

The major component of the delivery system for the high pressure water to the cleaning nozzles is a horizontal triplex plunger pump. The pump is powered by a 40 hp, 460 volt, 60 Hz, 3 phase, electric motor via a multiple V-belt drive. The constant displacement pump produces the volume flow rate from a reciprocating action with close tolerance plunger diameters.

Complementing the high pressure triplex plunger pump is a low pressure (50 psig) filtered water supply to the pump, a starter and circuit breaker protection for the motor, a rupture disc relief protection for the pump, and high pressure valves and tubing for bypassing and control of the flow from the pump. Figure 2 is a photograph of the test facility. Low pressure (50 psig) water is supplied to the high pressure horizontal triplex plunger pump through a conventional water supply source.

This flow can also be diverted to fill an environmental chamber for controlled condition testing of the cavitating nozzles or to fill a test tank for evaluation of cleaning rates. The water supply pressure to the pump is monitored to maintain a required positive suction head for effective operation of the force feed water lubricators. The flow through the high pressure nozzle is regulated by the nozzle pressure control and the nozzle bypass valve. Pressure gauges located at the discharge of the pump monitors the pressure developed at the nozzle.

## 2.2 Control and Instrumentation Subsystem

The pumping system has a standard shunt-switch electric control and an auxiliary power control. The control panel consists of various pressure gauges for nozzle and suction pressure in addition to specific pressure gauges for the environmental test chamber. The chamber pressure gauges are designated low range (0-160 psi), mid range (0-600 psi), and high range (0-1,500 psi) for accurate monitoring of the environmental tests. Independent controls are associated with each pressure indicator for gauge protection against excessive pressures. The flow meter control and the chamber pressure control actuate the flow meter and pressure gauges. The critical operating parameters can be monitored from the central control panel and the necessary functions can be performed in order to determine the loss coefficient measurements and to gather engineering data on specific nozzle designs.

### 2.3 Nozzle Performance and Fouling Removal Evaluation

#### Subsystem

Evaluation of loss coefficients and other measures of performance for the cavitating nozzles were conducted from a controlled environment test chamber. The design of the test chamber required proper location of the jet nozzle and standard test material in order to establish cavitation parameters. The nozzle and test material location were designed and incorporated into the environmental test chamber with a variable distance capability. The chamber has a pressure capability of 1,500 psi, a test material size capability of 6" x 6" x 2", an offset distance capability of 9" and view ports for cavitation erosion and intensity determination from bubble formation. The chamber permits visual and quantitative analysis of cavitating jets. The flexibility of this chamber makes possible the evaluation of many different types, sizes, and configurations of nozzles in terms of velocity, efficiency, and intensity for varying operating pressure conditions and nozzle standoff distances. Additionally, the chamber allows for the determination of erosion resistance of materials to cavitating jets.

Evaluation of the fouling and coating removal technique is accomplished through a large test tank and two test stands. Figure 3 shows the test tank and cleaning rate mechanism which permits a series of experiments to determine cleaning rate data. Optimum coating removal rates for different degrees of fouling



with various nozzle configurations and velocities have been determined. The capability exists to vary the speed at which the fouled test panels are moved past the stationary nozzle. The nozzle is rigidly attached to the cleaning rate mechanism. The fouled plate as shown in Figure 4 is clamped to a movable carriage, which can attain a maximum translation rate of 15 in./sec. Along with the capability to vary the operating pressure of the cavitating nozzle in the large test chamber, the effects of different nozzle diameters on the cleaning rates were also evaluated

The width of "cut" for the nozzles varied from a maximum of 3 inches to a minimum width of 5/16 inch. The width of the "cut" was directly dependent on the operation being performed. A 3 inch width was realized in an operation that was designed to remove only the fouling from the epoxy vinyl coated test specimens. The operation that yielded the 5/16 inch width was derived to remove the fouling as well as the epoxy vinyl coating. The latter operation brought the steel substrate to bare metal.

### 3.0 EXPERIMENTAL RESULTS AND DISCUSSION

The objective under this initial laboratory research program was to ascertain the technical feasibility of utilizing cavitation to remove the protective coating including the marine growth and fouling from test panels. The feasibility of utilizing a cavitating water jet cleaning system for removing marine growth from offshore platforms was demonstrated under laboratory conditions. Marine growth and barnacles were removed from the test specimens exposing the steel substrate.

#### 3.1 Program Approach

Initially, two orifice sizes were evaluated which consisted of an 0.042 inch diameter and a 0.047 inch diameter nozzle. Additionally, two swirl inducers, #45 and #46 were also evaluated. These swirl inducers in combination with the two nozzle sizes provided six nozzle configurations that were evaluated.

An experimental test facility was designed and calibrated for this program. A high pressure triplex plunger pump was utilized in these initial evaluations. A panel which contains valves to regulate the flow produced by the pump as well as high range and low range pressure gauges to monitor the pressures was constructed.

A cleaning rate mechanism was also constructed. The fouled test specimen was mounted on a movable carriage which translates the plate across a stationary nozzle assembly. A variable speed motor controls the translation rate which may attain a maximum value of 15 in./sec. As the fouled specimen moves across the



stationary nozzle assembly, the cavitating jet impinges on the surface of the test specimen and removes all of the accumulated marine growth and fouling including the protective coating thereby exposing the steel substrate.

### 3.2 Initial Nozzle Configurations

The necessary experimental studies were undertaken and design data was generated to define the specific design parameters associated with the cavitation platform cleaning technique. The nozzle sizes initially chosen for this program were an 0.042 and an 0.047 inch diameter nozzle. After conducting evaluations of these nozzle designs and reducing the accumulated data, smaller orifice sizes were tested because these nozzles indicated poor operating performance. The nozzle sizes chosen were a 0.031 inch diameter and a 0.023 inch diameter nozzle. The performance of these nozzles exceeded the performance of the 0.042 inch and 0.047 inch diameter nozzles.

### 3.3 Operating Parameters

The operating parameters that were investigated in this program included: 1) loss coefficient, 2) intensity of erosion, 3) cleaning rate, and 4) horsepower utilized.

#### 3.3.1 Loss Coefficient

Figure 5 is a comparison of the loss coefficient ( $C_v$ ) performance of the two nozzle diameters that were originally evaluated in the program. The  $C_v$  data depicted in the figure is for the 0.042 inch and 0.047 inch diameter conical nozzles without

the swirl inducers.  $C_v$  data was gathered for a pressure range from 1,000 psi through 7,000 psi. The  $C_v$  values were nominally 0.74 for the 0.047 inch nozzle and 0.55 for the 0.042 inch diameter nozzle. These  $C_v$  values indicate that the 0.047 inch nozzle is a more efficient nozzle design than the 0.042 inch nozzle. The loss coefficient is a comparison of the actual velocity of the water through the nozzle to the theoretical velocity predicted for the nozzle size at some discrete pressure level of interest. The data shows the 0.047 inch nozzle is approximately 20% more efficient throughout the entire pressure range than the 0.042 inch nozzle.

The effects on  $C_v$  for adding swirl inducers to the two nozzle designs is shown in Figures 6 and 7. Two swirl inducers were evaluated, #45 and #46. The #45 swirl inducer imparts a more vigorous swirl to the flow passing through the nozzle. This results in a decrease in the loss coefficient for any nozzle using the #45 swirl. This can be seen in the figures for both the 0.042 inch and 0.047 inch nozzle. For the 0.042 inch nozzle, Figure 6, the  $C_v$  values are decreased to 0.50 from 0.55 in the non-swirl configuration. In Figure 7, the  $C_v$  values for the 0.047 inch nozzle with the #45 swirl are nominally 0.57. This is a much lower value than the  $C_v$  for the nozzle without a swirl 0.74.

Additional  $C_v$  data was gathered using the #46 swirl in both nozzles. When the #46 swirl is utilized, slight increases in

the  $C_v$  values are realized. This indicates that the nozzles using the #46 swirl inducer are more efficient than the same size nozzle in a non-swirl configuration.

### 3.3.2 Intensity of Erosion

The next step after collecting the  $C_v$  data is to evaluate the intensities of erosion produced by the various nozzle configurations at several nozzle distances. These measurements are made using the intensity test stand. An aluminum test plate is affixed in the stand, and the time that is required for the jet to break through the plate at some specific pressure level and nozzle distance is recorded. From this information, the intensity vs. nozzle distance curve can be constructed.

Figure 8 contains intensity data for the 0.042 inch nozzle in a non-swirl configuration at three pressure levels: 3,000; 5,000; and 7,000 psi. At 7,000 psi the maximum intensity of erosion is 2,400 watts/meter<sup>2</sup>. This maximum value occurs at a nozzle distance of 0.5 inch.

In Figures 9 and 10 the effects of swirl inducement on the intensity produced by the 0.042 inch nozzle is shown. It has been discovered that by inducing a swirl in a nozzle, the optimum nozzle distance is decreased. With swirls the intensities produced are approximately the same as the non-swirl nozzle, however, at a decreased nozzle distance. Figure 9 shows the intensity data with the #46 swirl. At 7,000 psi the maximum intensity produced is 2,900 watts/meter<sup>2</sup>. This occurs at a



nozzle distance of 0.125 inch which is less than the 0.5 inch nozzle distance of the non-swirl nozzle.

Figure 10 shows the 0.042 inch nozzle with the #45 swirl. The severity of the #45 swirl decreases the optimum nozzle distance still further. The optimum nozzle distances are now less than 0.1 inch.

Figures 11 through 13 are the intensity vs. nozzle distance data for the three configurations of the 0.047 inch nozzle. Figure 11 shows the non-swirl configuration of the nozzle. At 7,000 psi the maximum intensity generated is 6,200 watts/meter<sup>2</sup> at a nozzle distance of 1.0 inch. At 5,000 psi with this nozzle configuration, the intensity of erosion produced by the 0.047 inch nozzle is equal to the intensity of erosion produced by the 0.042 inch nozzle at 7,000 psi.

In Figures 12 and 13 the effects of swirl on the 0.047 inch nozzle are shown. As was discussed previously with the 0.042 data, the swirls decrease the optimum nozzle distance yet maintain the same intensity levels as a nozzle without a swirl. With the #46 swirl, the optimum nozzle distance is less than 0.1 inch at 7,000 psi; and with the #45 swirl in Figure 13, the optimum nozzle distance is less than 0.05 inch.

### 3.3.3 Cleaning Rate Data

After gathering the intensity and loss coefficient data, the performance of the individual nozzle configurations was analyzed so the most effective nozzle design could be chosen

to be used in cleaning rate evaluations. During this analysis it became evident that using smaller orifice diameters incorporated with higher pressures would yield significantly greater cleaning rates. Additionally, it became evident that the intensity envelope produced through the utilization of the swirls does not allow for a deviation from the optimum nozzle distance before the maximum intensity values decreased rather sharply. However, a nozzle design with that critical a dependence on distance would be difficult to use, effectively in a field operation.

#### 3.3.3.1 Nozzle Diameter Determination for Cleaning Rate Data

One of the design goals of the program was to remove all fouling from the test panels and to clean the panel to bare metal. Initial cleaning rate trials utilizing the 0.042 and 0.047 nozzle configurations yielded very poor results. These nozzles were unable to clean the test specimen to a bare metal condition. Higher pressures could not be used with these nozzles due to the flow limitations of the high pressure pump in the laboratory. Therefore, to achieve the higher pressures that would enable the fouling to be removed and clean the plates to bare metal, it was necessary to decrease the diameter of the nozzles. In this manner the high pressure of 14,000 psi was achieved and the flow capabilities of the pumping system were not exceeded. The two nozzle sizes chosen for



evaluations were a 0.023 inch diameter and a 0.031 inch diameter. The standard calibrations were performed on these new nozzle configurations. Loss coefficient data for the 0.023 inch nozzle is shown in Figure 14. In the non-swirl condition the  $C_v$  was nominally 0.665. When the #46 swirl was added to the nozzle, the efficiency was slightly higher--0.675. The #45 swirl reduced the  $C_v$  to 0.65. Figure 15 is the loss coefficient performance of the 0.031 inch nozzle. The #45 swirl, as was stated before, produces a more intense swirl; therefore, a nozzle in this configuration has a lower efficiency. For the 0.031 inch nozzle with the #45 swirl the  $C_v$  is nominally 0.66. With no swirl the  $C_v$  rises to 0.79, and with the #46 swirl the  $C_v$  rises still higher to a nominal value of 0.815.

Intensity data for the 0.023 inch and 0.031 inch diameter nozzles is contained in Figures 16 and 17. Figure 16 is the intensity of erosion ( $I_e$ ) as a function of nozzle distance for three configurations of the 0.023 inch nozzle at an operating pressure of 14,000 psi. The maximum  $I_e$  produced by this nozzle, 15,000 watts/meter<sup>2</sup>, at the specified pressure level occurred in the non-swirl configuration at a nozzle distance of 0.5 inch. When the swirl inducers were added to the nozzle, the optimum nozzle distance decreased. The #46 swirl decreased the nozzle distance to 0.125 inch. The maximum  $I_e$  for this configuration was 8,300 watts/meter<sup>2</sup>. The #45 swirl produces a more vigorous swirl than the #46 swirl. Therefore, the #45 swirl produces a

less intense jet, due to higher energy losses in the nozzle, at a lower optimum nozzle distance. The optimum nozzle distance is less than 0.0625 inch at an  $I_e$  of 5,600 watts/meter<sup>2</sup>.

Figure 17 contains the  $I_e$  as a function of nozzle distance information for the 0.031 inch nozzle. The non-swirl condition of this nozzle produces a maximum  $I_e$  of 12,100 watts/meter<sup>2</sup> at a distance of 0.5 inch. When the #46 swirl inducer is attached to the nozzle, the optimum nozzle distance decreases to 0.25 inch. The  $I_e$  at this point is 14,600 watts/meter<sup>2</sup>. Finally, the last configuration of the 0.031 nozzle, the #45 swirl, produces an  $I_e$  of 6,300 watts/meter<sup>2</sup> at a nozzle distance of 0.0625 inch.

#### 3.3.3.2 Threshold Intensity of Erosion for

##### Barnacles and Steel Substrate Material

Before proceeding into the cleaning tests, it was imperative that the threshold values for the barnacles and substrate material be determined so that the parameters governing jet intensity could be adjusted to yield an intensity that would remove the fouling, yet not damage the steel surface. The threshold intensity for removing barnacles was determined to be 448 watts/meter<sup>2</sup> as shown in Figure 18. This is substantially less than the intensity required to remove the platform structure material (20,000 watts/meter<sup>2</sup>) which implies that fouling can easily be removed without damage to the substrate.

### 3.3.3.3 Cleaning Rate Data Tests

At this stage in the test program, samples of fouled plates were obtained to be used in the cleaning rate determinations. These heavily fouled plates were submerged in the Atlantic Ocean for several months.

The measured power output and cleaning rate as a function of nozzle diameter is presented in Figure 19. The 0.023 inch diameter nozzle with a #46 swirl insert at 14,000 psi cleaned at a rate of 9.4 ft<sup>2</sup>/hr. Removing the swirl insert increased the cleaning rate to 12.5 ft<sup>2</sup>/hr. The 0.031 inch diameter nozzle provided higher cleaning rates. With a #46 swirl insert at 14,000 psi, a cleaning rate of 14.1 ft<sup>2</sup>/hr. was achieved.

### 3.4 Horsepower Requirements

The horsepower utilized for the 0.031 nozzle with a #46 swirl was 24.7 hp. When no swirl was used, the horsepower was decreased to 22.4 while the cleaning rate was increased to 15.6 ft<sup>2</sup>/hr. (37.5 in<sup>2</sup>/min.). The plates were cleaned of all fouling and protective coating down to the steel surface. The CONCAVER<sup>TM</sup> cleaning technique removed the fouling and exposed the steel substrate.

Figure 20 shows a heavily fouled test panel partially cleaned utilizing the CONCAVER<sup>TM</sup> cleaning technique. Marine growth and the protective coating were completely removed from the plate at a rate of 16 ft<sup>2</sup>/hr. exposing the steel substrate to bare metal.



#### 4.0 CONCLUSIONS AND RECOMMENDATIONS

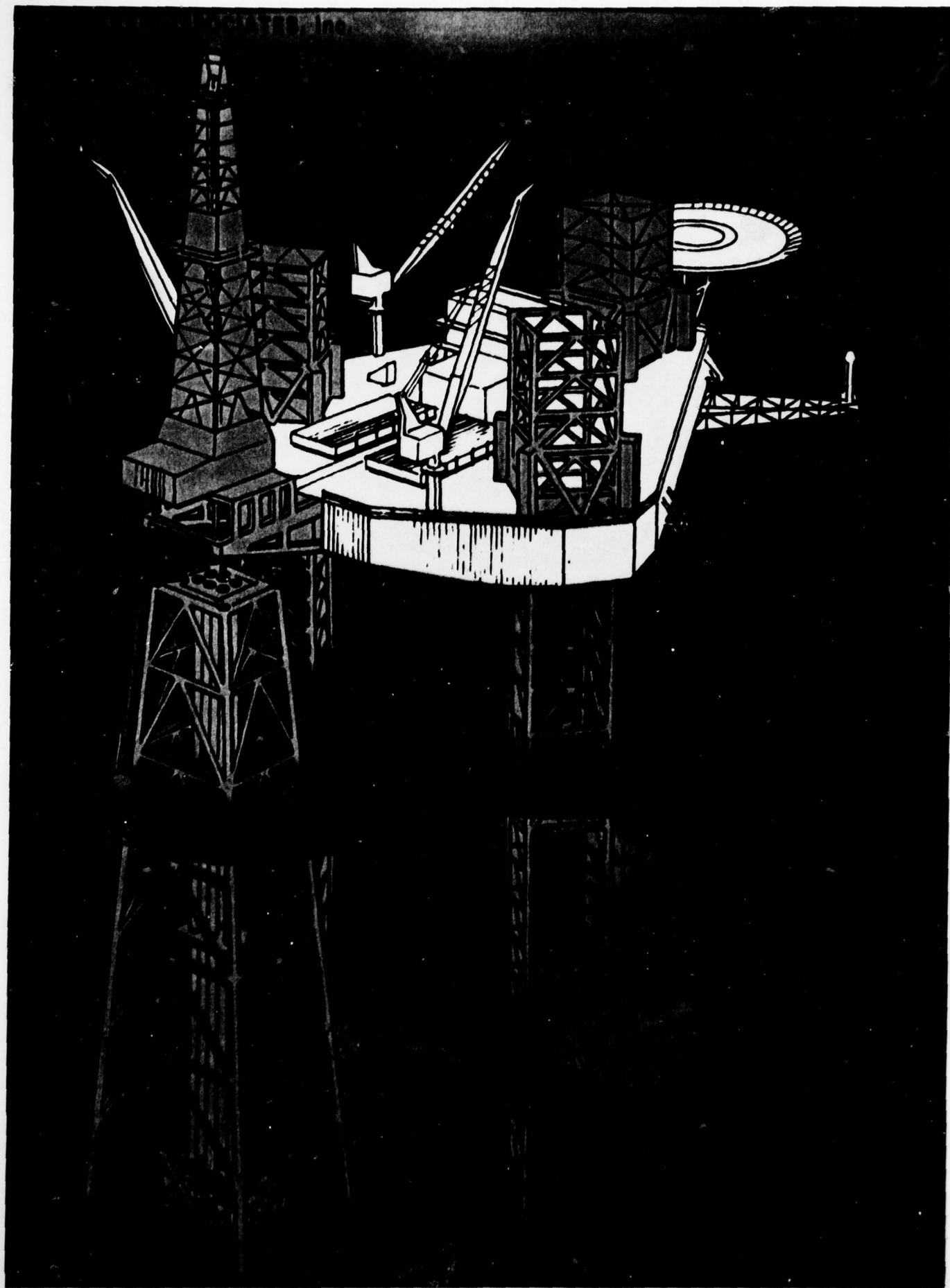
The research conducted in the present program has demonstrated the feasibility of using cavitating water jets to remove the fouling and protective coating to bare steel from test panels under laboratory conditions. The CONCAVER<sup>TM</sup> technique removed all of the fouling from the test panels without damaging the steel substrate.

For the 0.031 inch nozzle without swirl at an operating pressure of 14,000 psi, the cleaning rate was 15.6 ft<sup>2</sup>/hr. The horsepower utilized at this pressure was 22.4 hp. The sample plates were cleaned of all fouling and protective coating.

For this nozzle design, the marine growth was removed throughout a range of nozzle distances from 0.20 to greater than 3.5 inches. With this range of operating distances, the dependency on maintaining a specific nozzle distance has been alleviated and, therefore, would be easily utilized under field conditions.

The results of this initial feasibility evaluation indicate that the various design parameters such as cleaning rates, area covered, nozzle size, jet velocity, pump pressure and flow rate, and horsepower requirements are properly characterized in order to optimize the preliminary system parameters and design specifications for a field system. It is recommended that a field demonstration be conducted utilizing the CONCAVER<sup>TM</sup> technology.





DAEDALEAN ASSOCIATES, Inc.

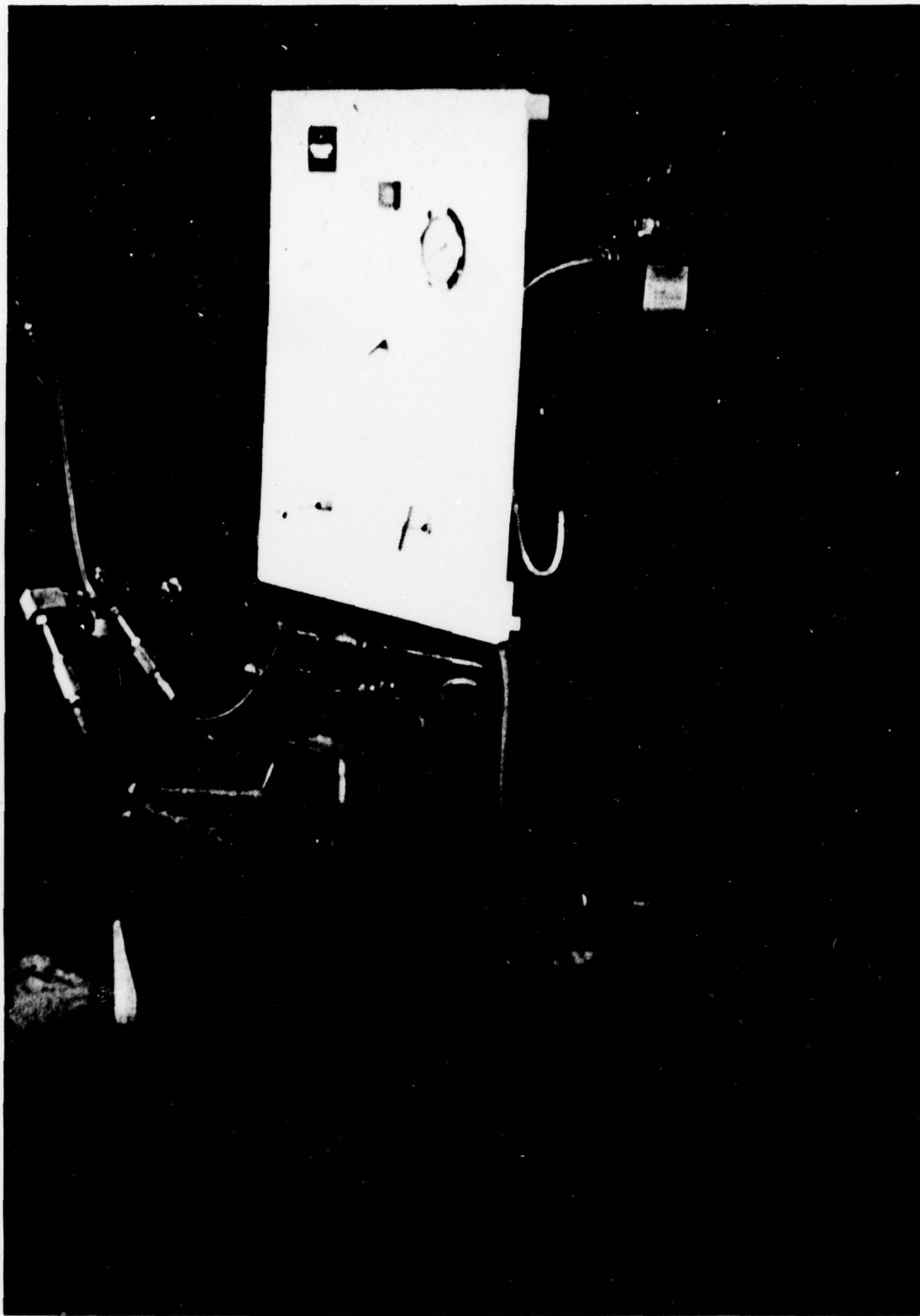
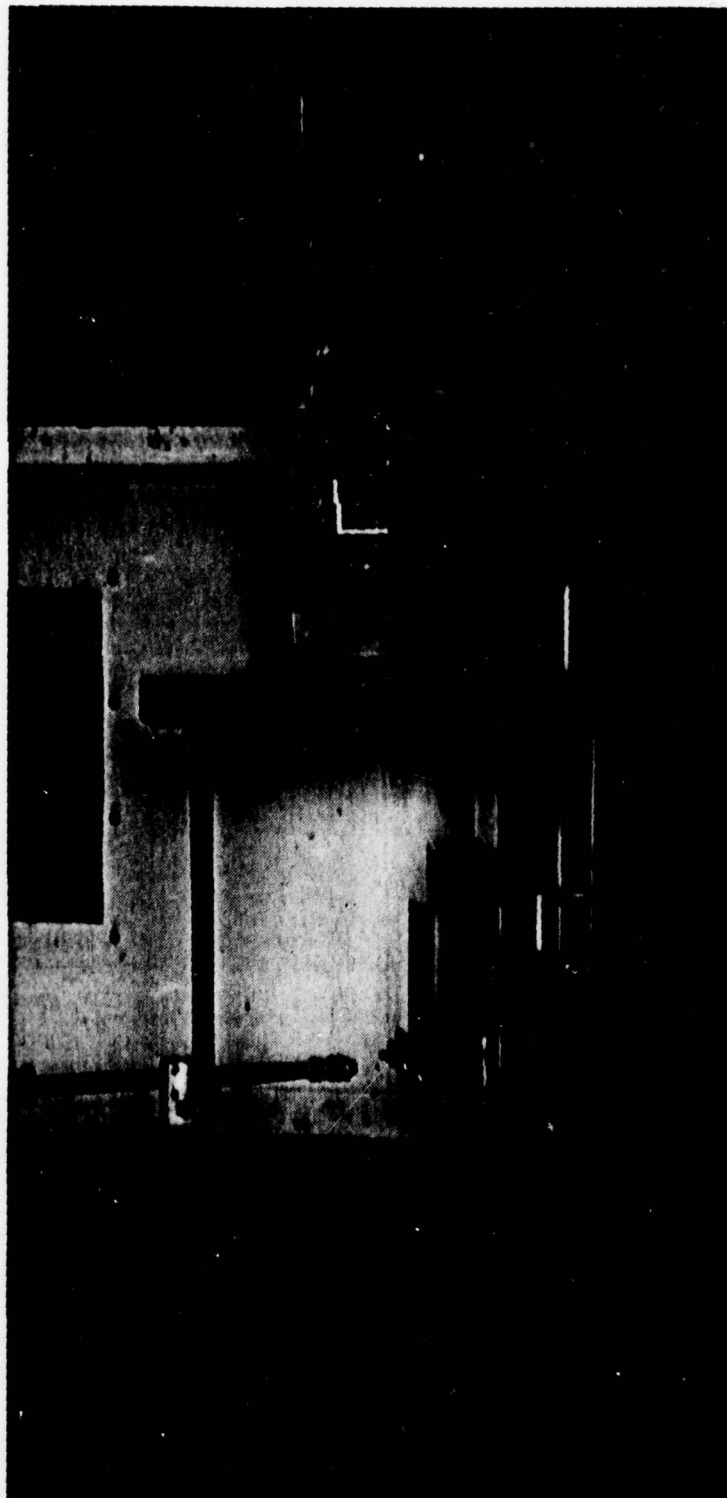


FIGURE 2 HIGH PRESSURE TRIPLEX PLUNGER PUMP

**DAEDALEAN ASSOCIATES, Inc.**



**FIGURE 3 DAI CLEANING RATE MECHANISM**

**DAEDALEAN ASSOCIATES, Inc.**

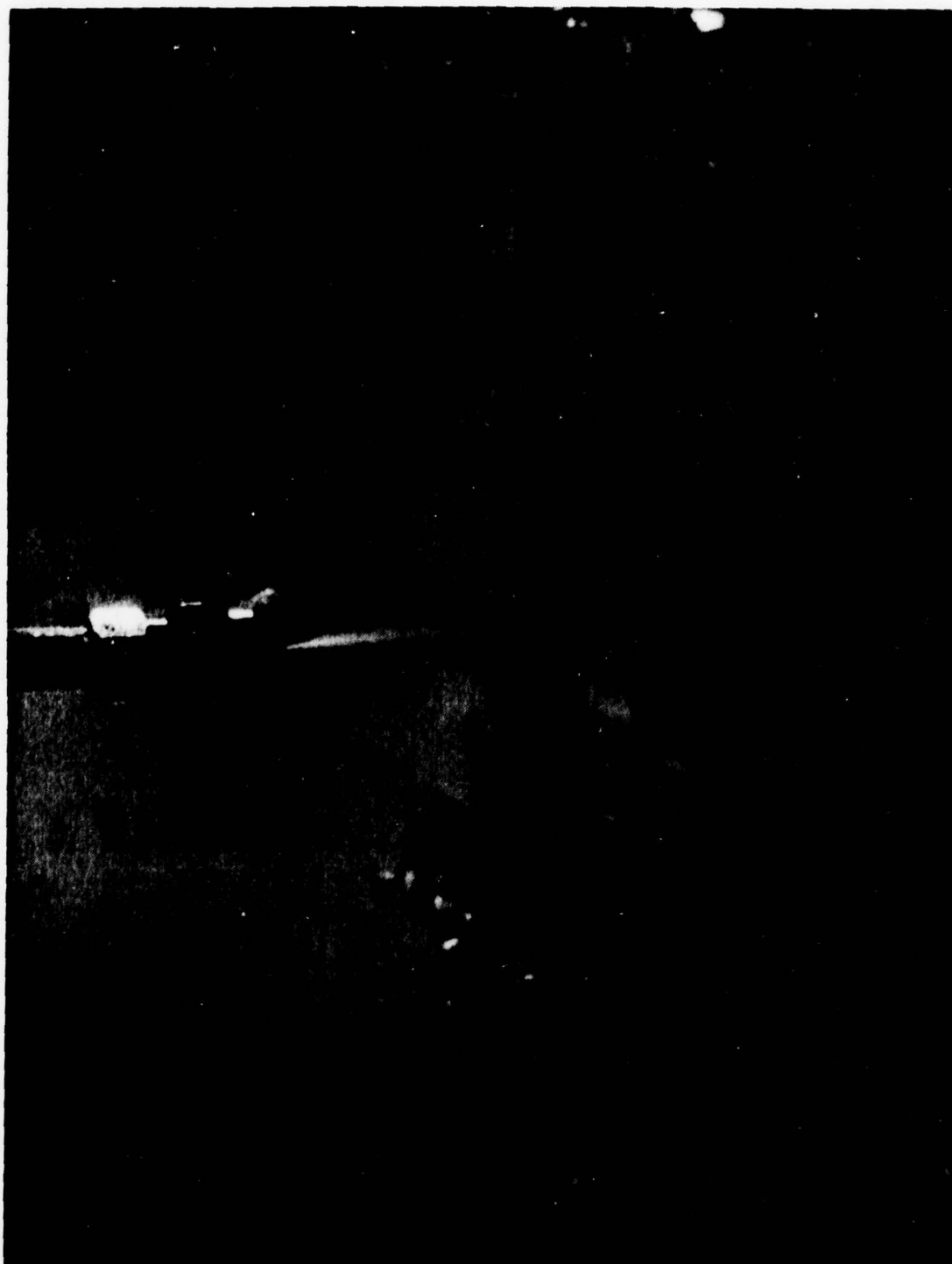


**FIGURE 4 FOULED PLATE BEING CLEANED UTILIZING  
CONCAVER TECHNIQUE**



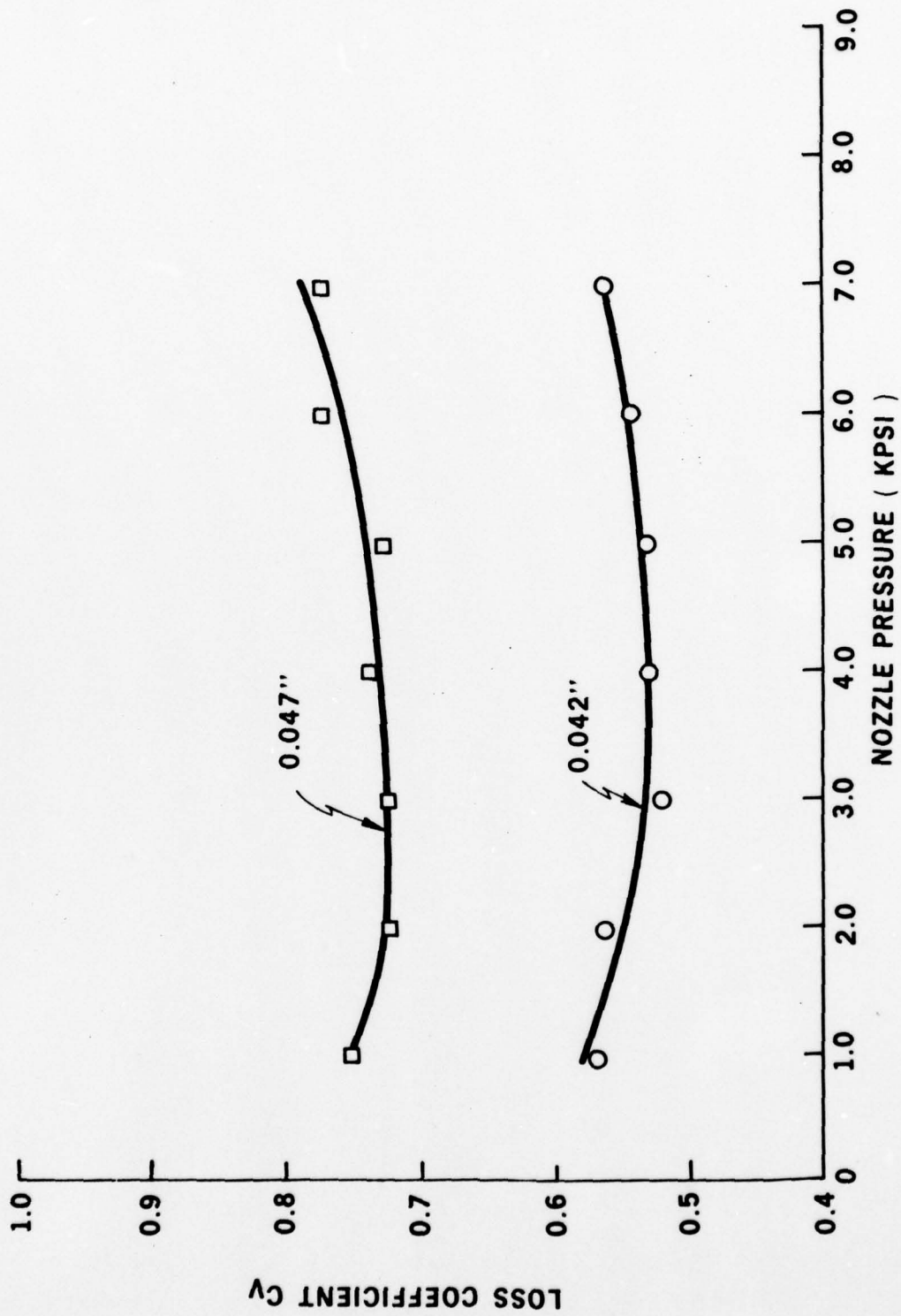


FIGURE 5 LOSS COEFFICIENT AS A FUNCTION OF NOZZLE PRESSURE FOR A SINGLE ORIFICE CONICAL NOZZLE

DAEDALEAN ASSOCIATES, Inc.

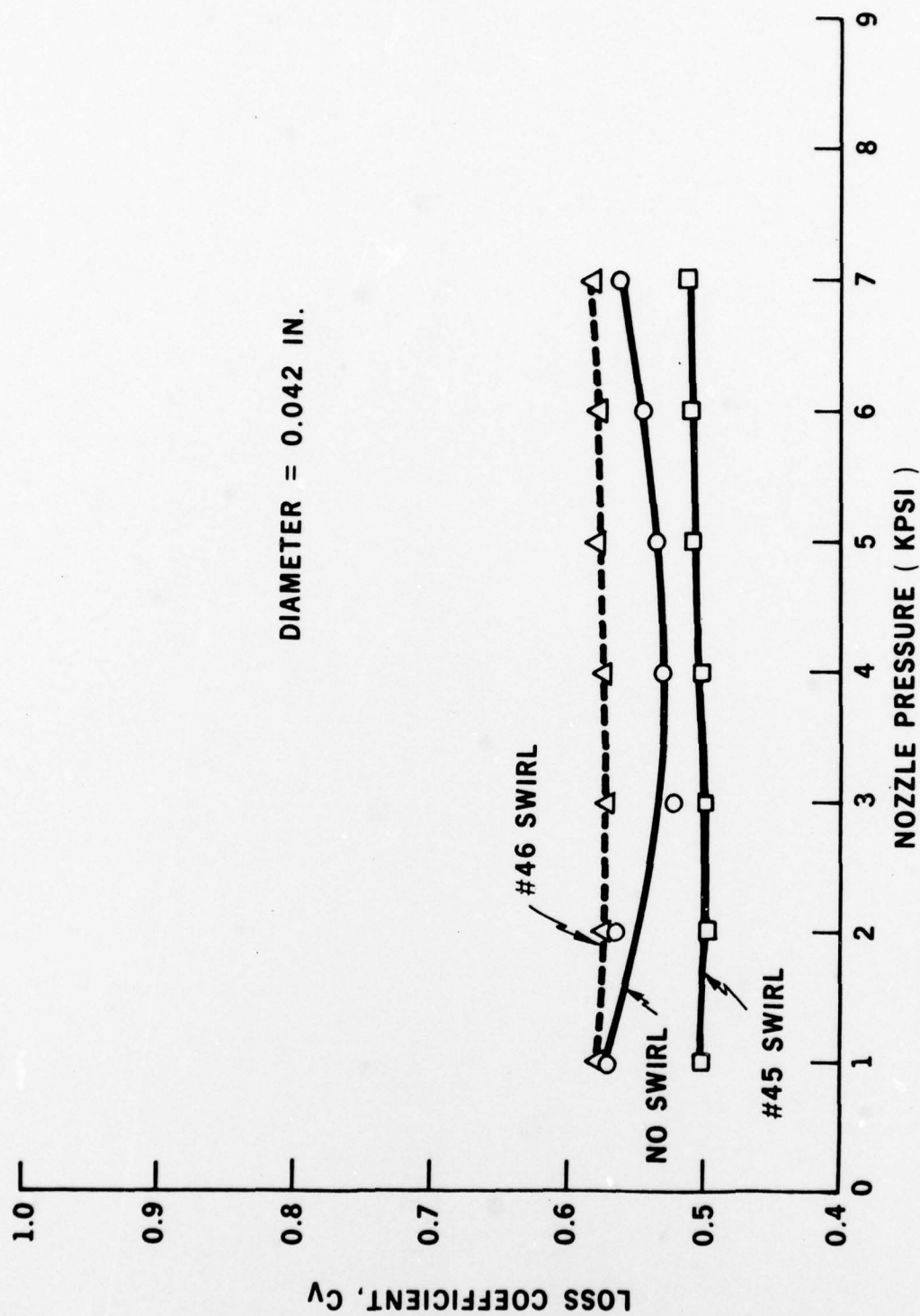


FIGURE 6 LOSS COEFFICIENT AS A FUNCTION OF NOZZLE PRESSURE FOR THREE CONFIGURATIONS OF THE 0.042 IN. DIAMETER ORIFICE NOZZLE

DAEDALEAN ASSOCIATES, Inc.

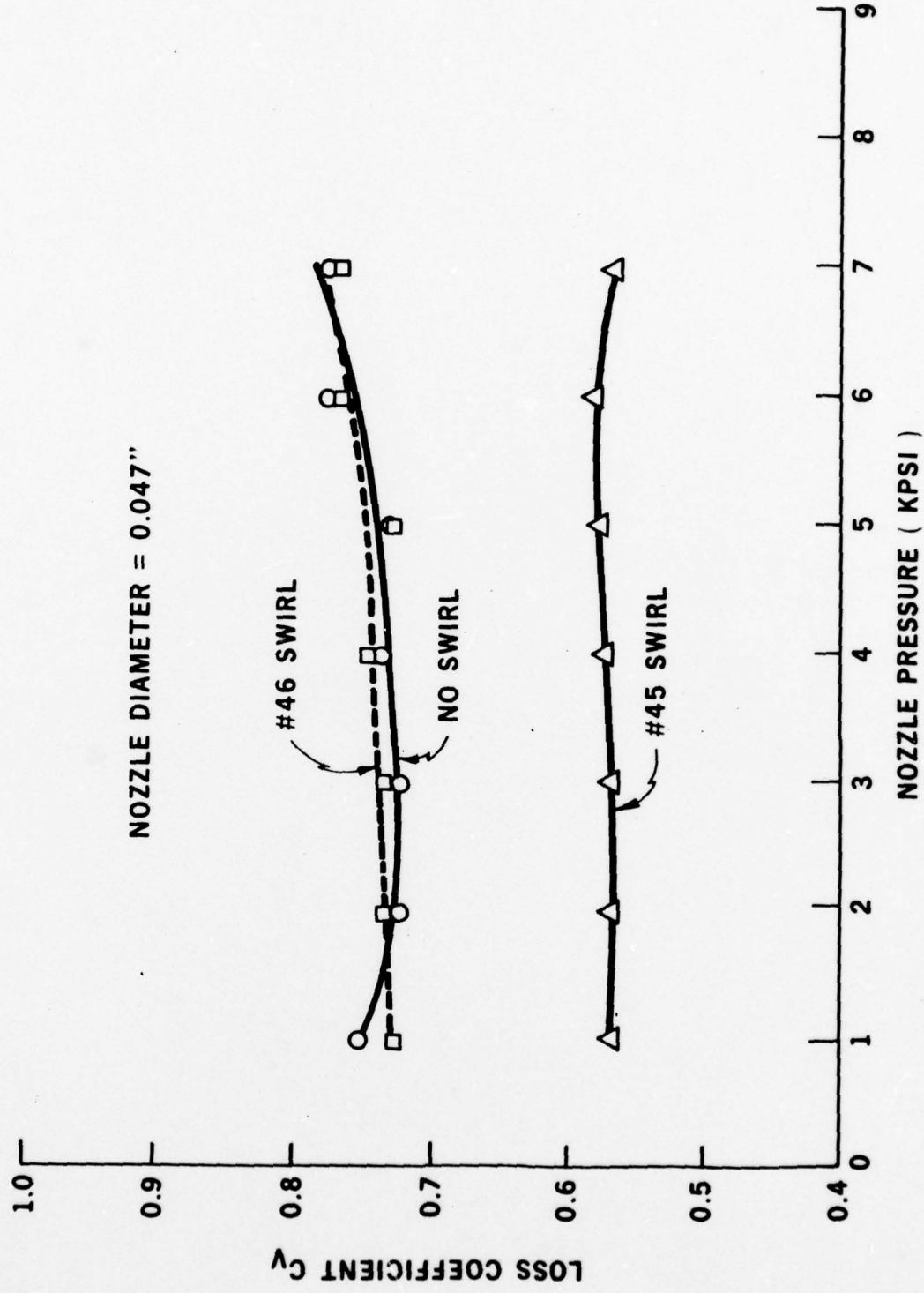


FIGURE 7 LOSS COEFFICIENT AS A FUNCTION OF NOZZLE PRESSURE FOR THREE CONFIGURATIONS OF THE 0.047 IN. DIAMETER NOZZLE

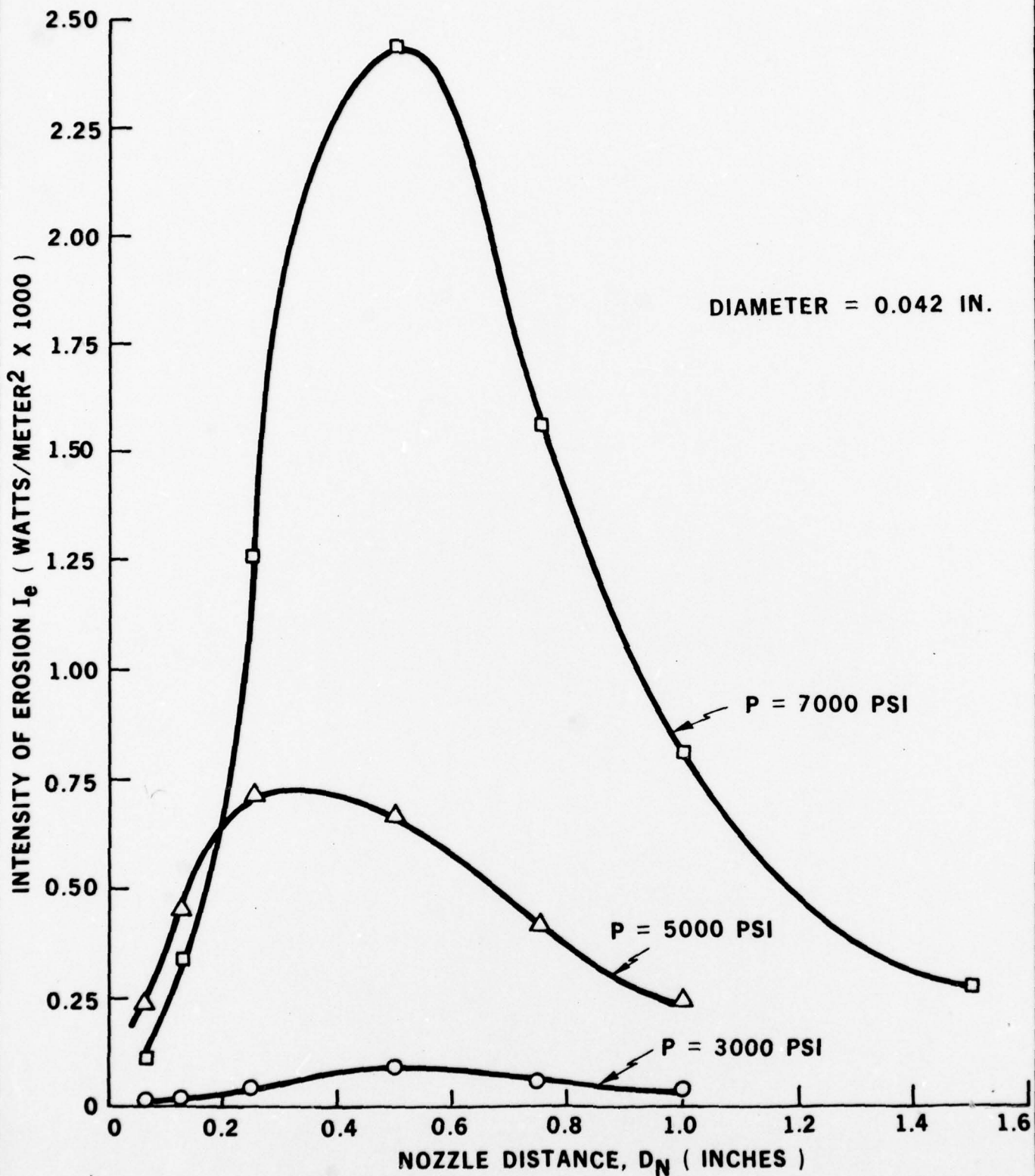


FIGURE 8 INTENSITY OF EROSION AS A FUNCTION OF NOZZLE DISTANCE FOR A 0.042 IN. DIAMETER NOZZLE WITH NO SWIRL AT THREE PRESSURES



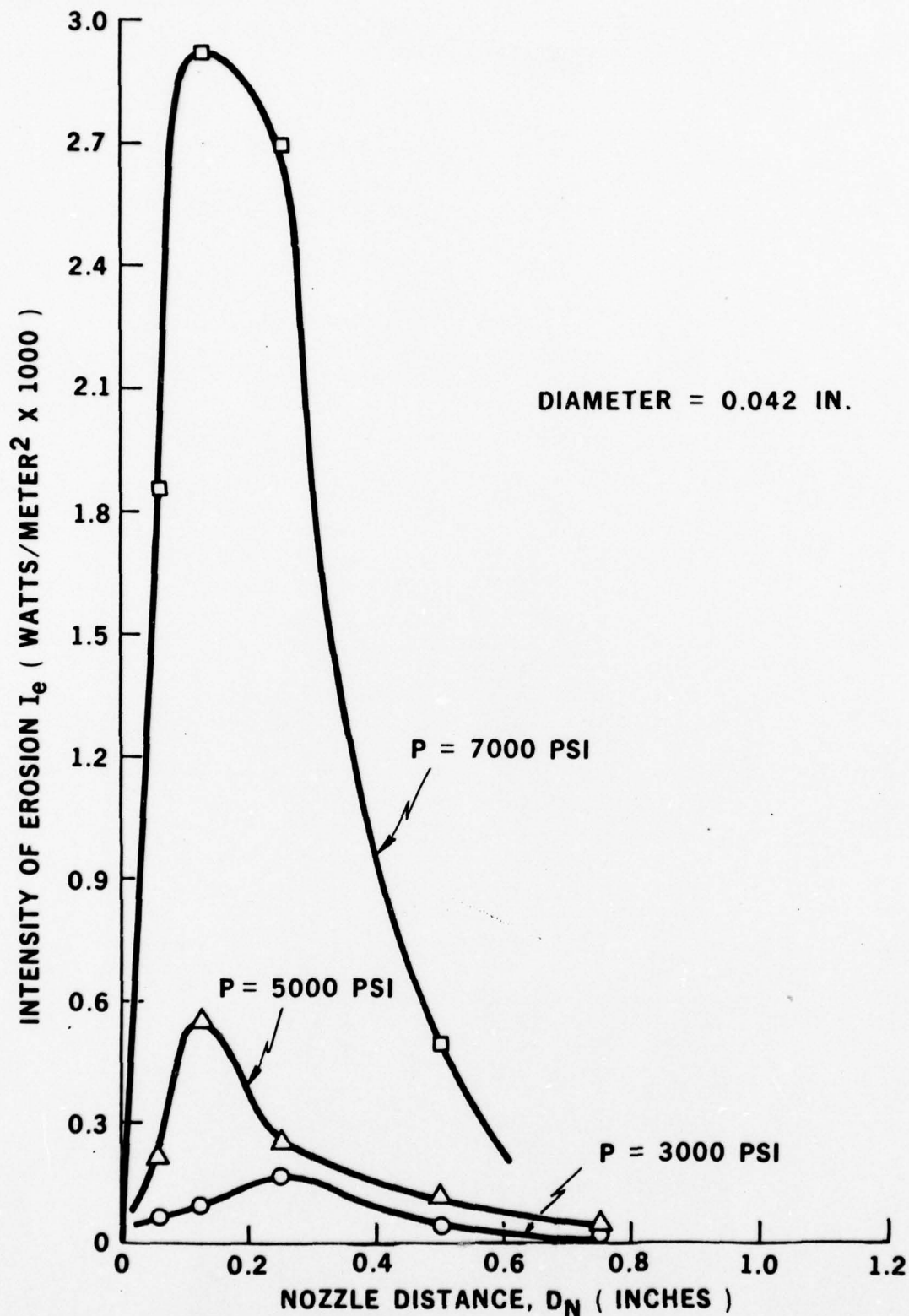


FIGURE 9 INTENSITY OF EROSION AS A FUNCTION OF NOZZLE DISTANCE FOR A 0.042 IN DIAMETER NOZZLE WITH A NUMBER 46 SWIRL INSERT AT THREE PRESSURES

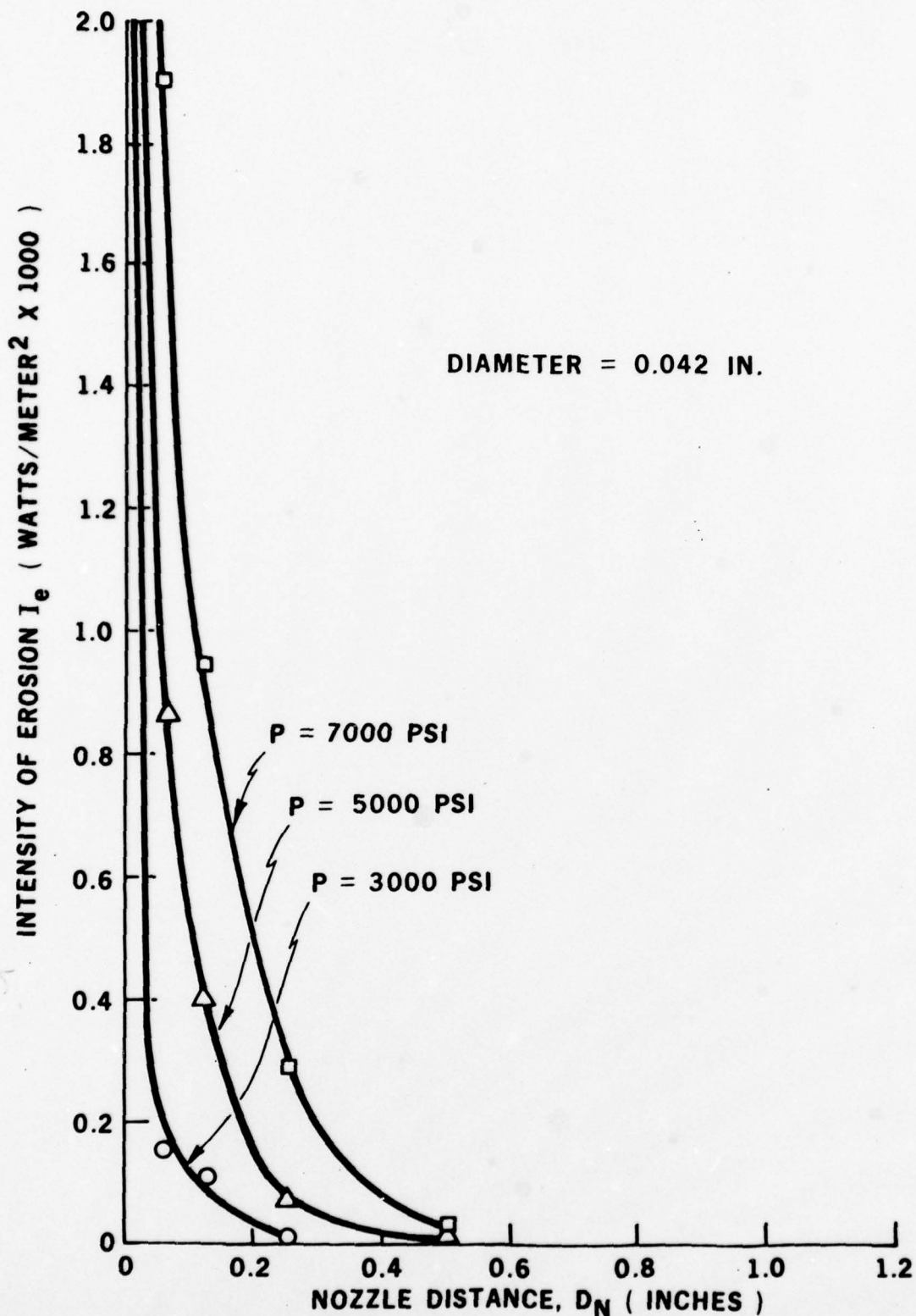


FIGURE 10 INTENSITY OF EROSION AS A FUNCTION OF NOZZLE DISTANCE FOR A 0.042 IN. DIAMETER NOZZLE WITH A NUMBER 45 SWIRL INSERT AT THREE PRESSURES

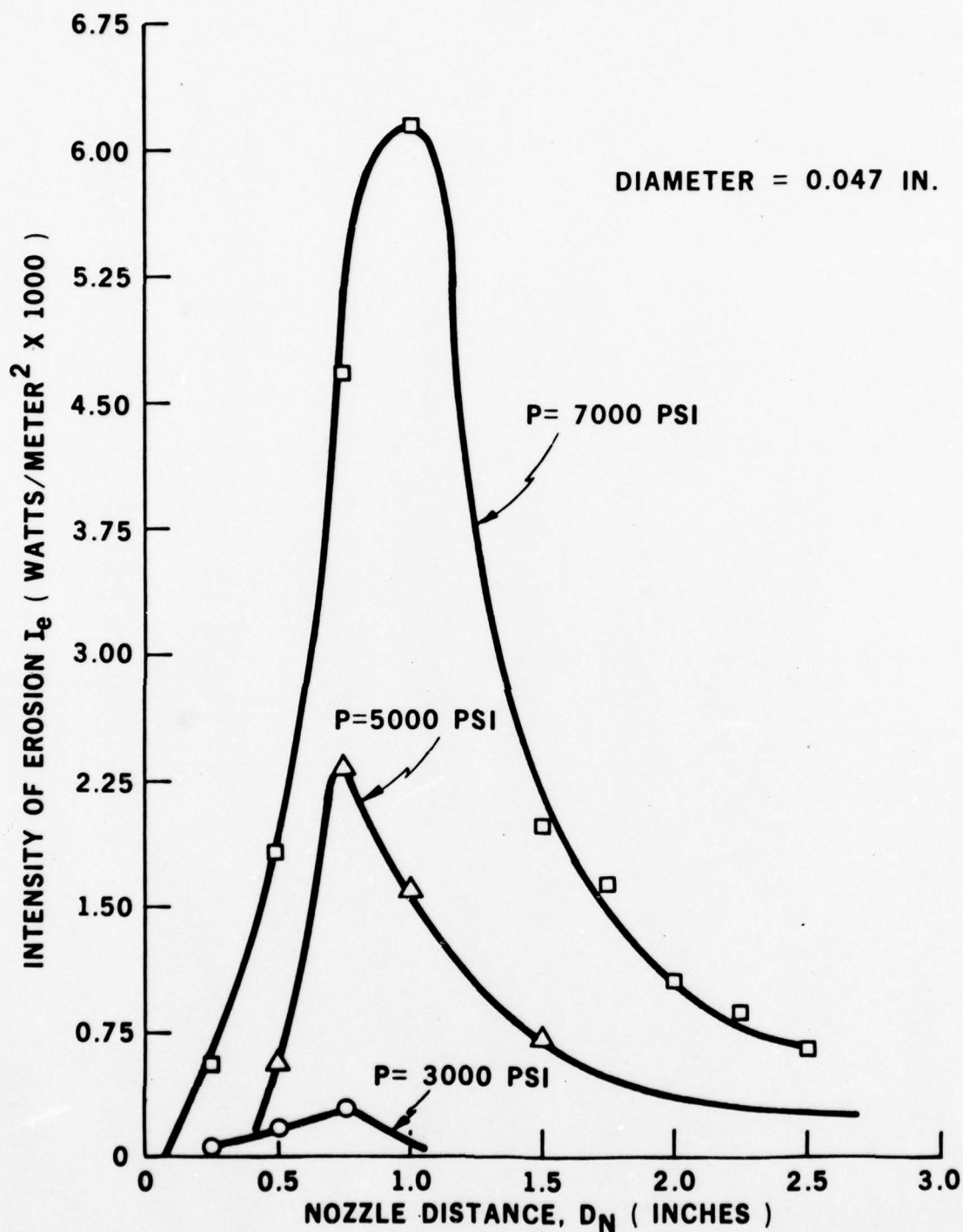


FIGURE 11 INTENSITY OF EROSION AS A FUNCTION OF NOZZLE DISTANCE FOR A 0.047 IN. DIAMETER NOZZLE WITH NO SWIRL INSERT AT THREE PRESSURES

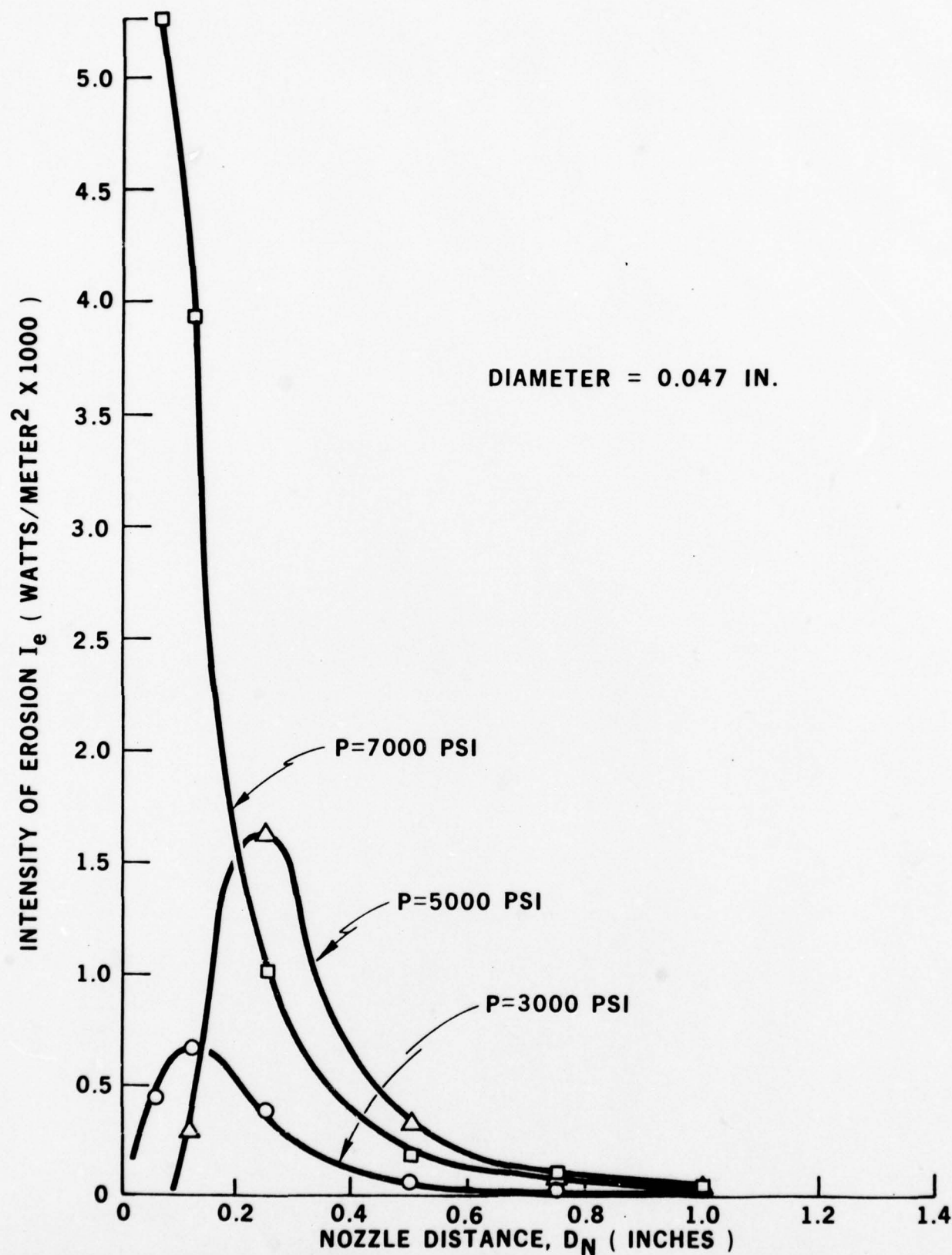


FIGURE 12 INTENSITY OF EROSION AS A FUNCTION OF NOZZLE DISTANCE FOR A 0.047 IN. DIAMETER NOZZLE WITH A NUMBER 46 SWIRL INSERT AT THREE PRESSURES



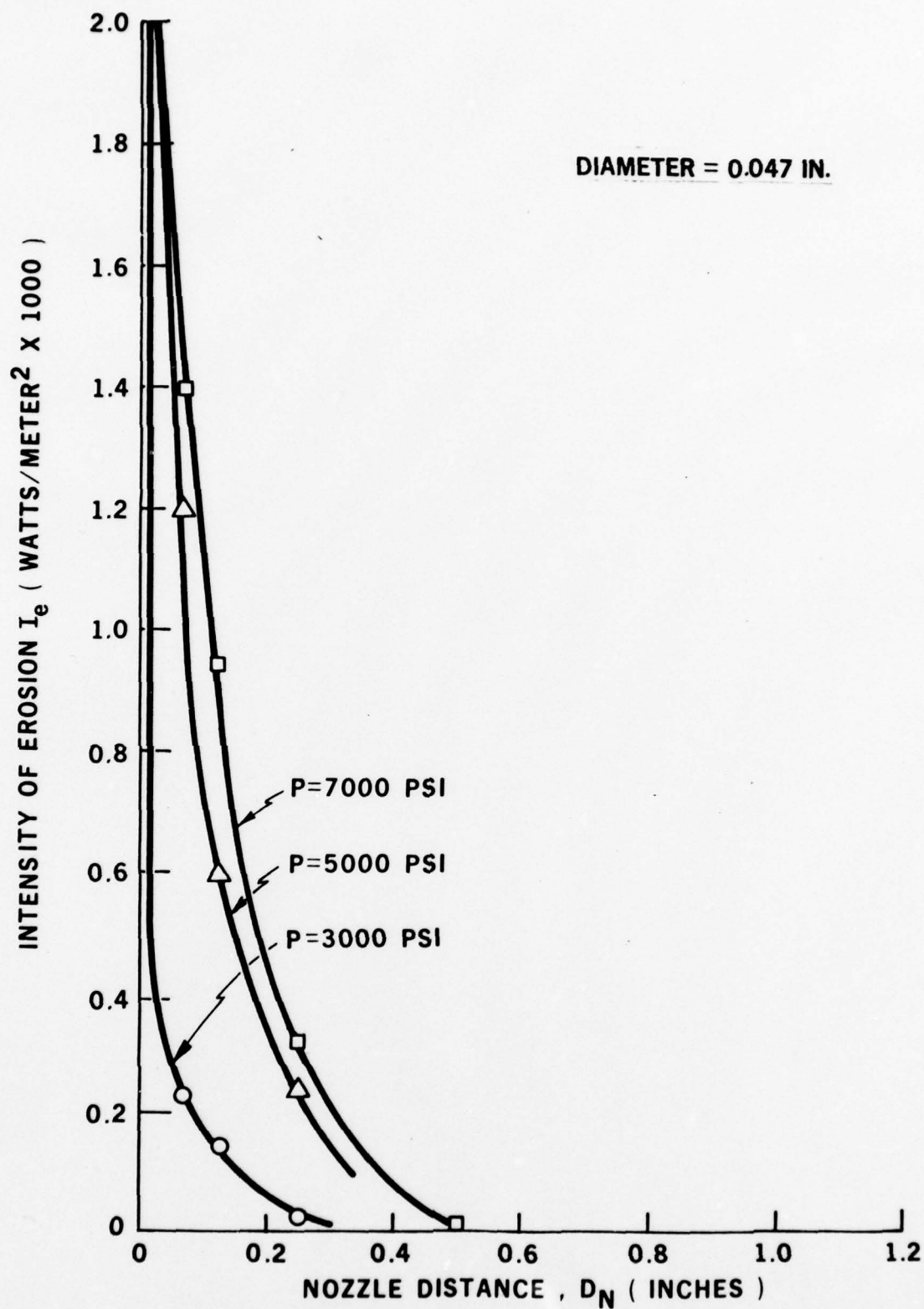


FIGURE 13 INTENSITY OF EROSION AS A FUNCTION OF NOZZLE DISTANCE FOR A 0.047 IN. DIAMETER NOZZLE WITH A NUMBER 45 SWIRL INSERT AT THREE PRESSURES

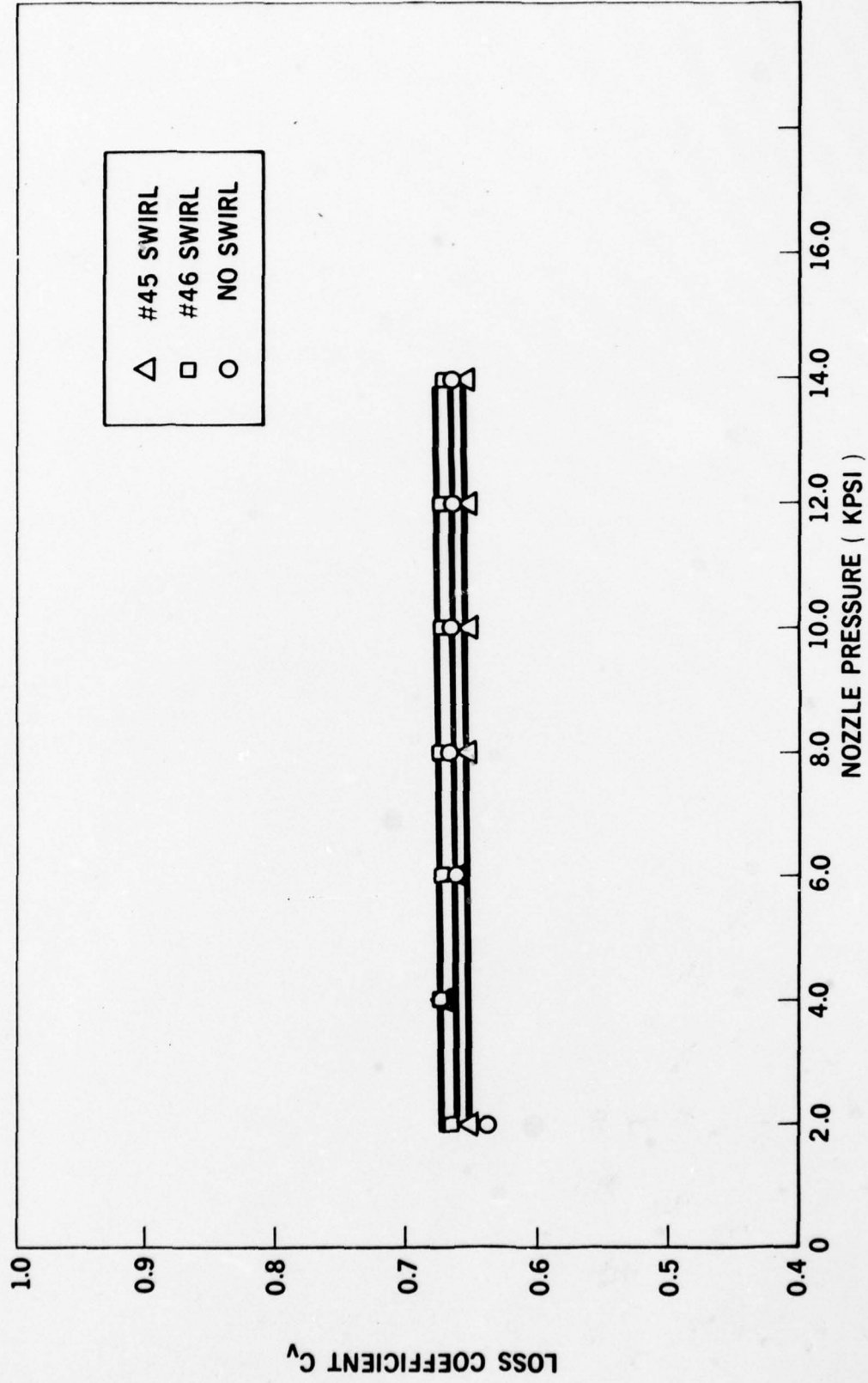


FIGURE 14 LOSS COEFFICIENT AS A FUNCTION OF NOZZLE PRESSURE FOR THREE CONFIGURATIONS OF THE 0.023 INCH DIAMETER NOZZLE

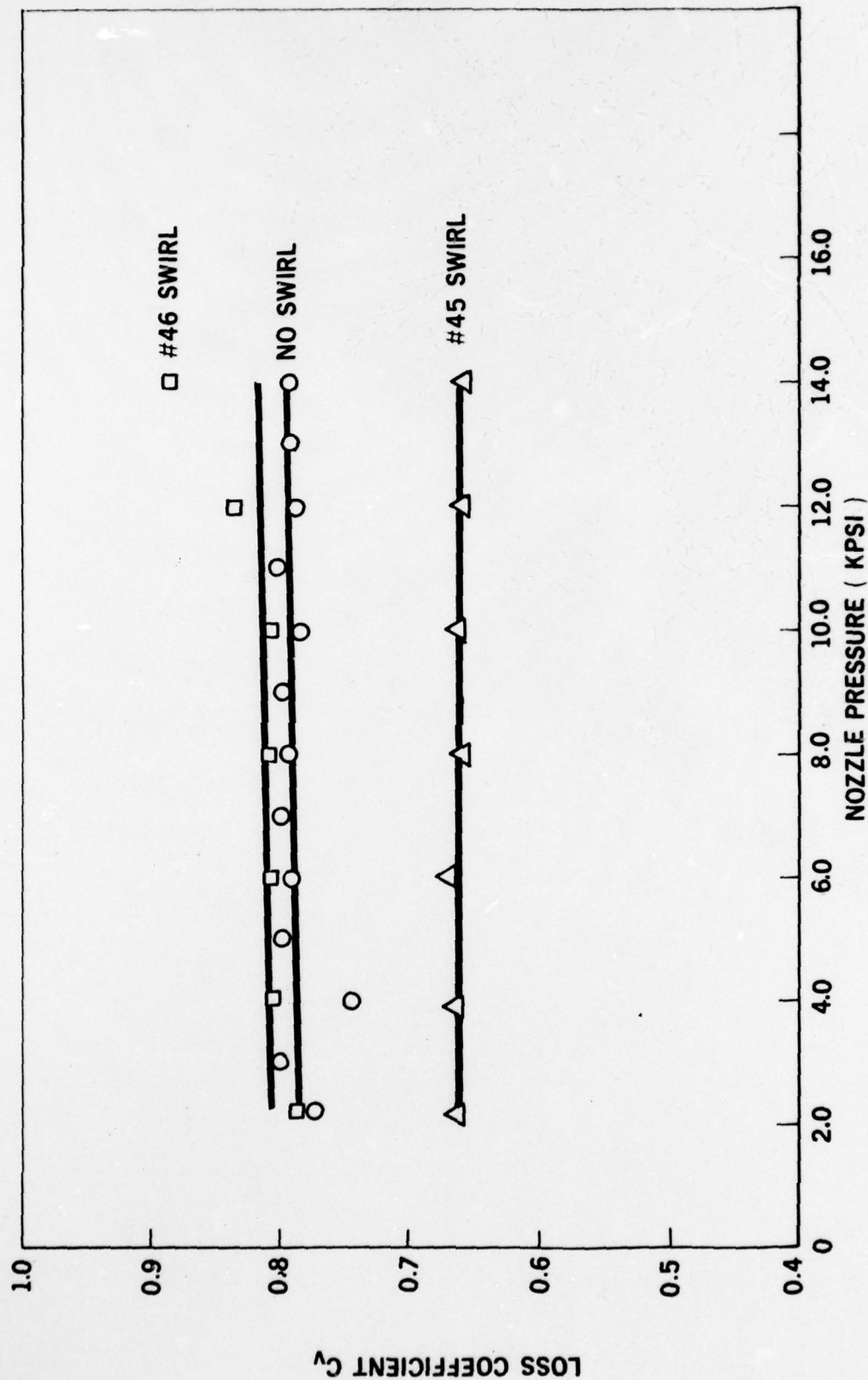


FIGURE 15 LOSS COEFFICIENT AS A FUNCTION OF NOZZLE PRESSURE FOR THREE CONFIGURATIONS OF THE 0.031 INCH DIAMETER NOZZLE

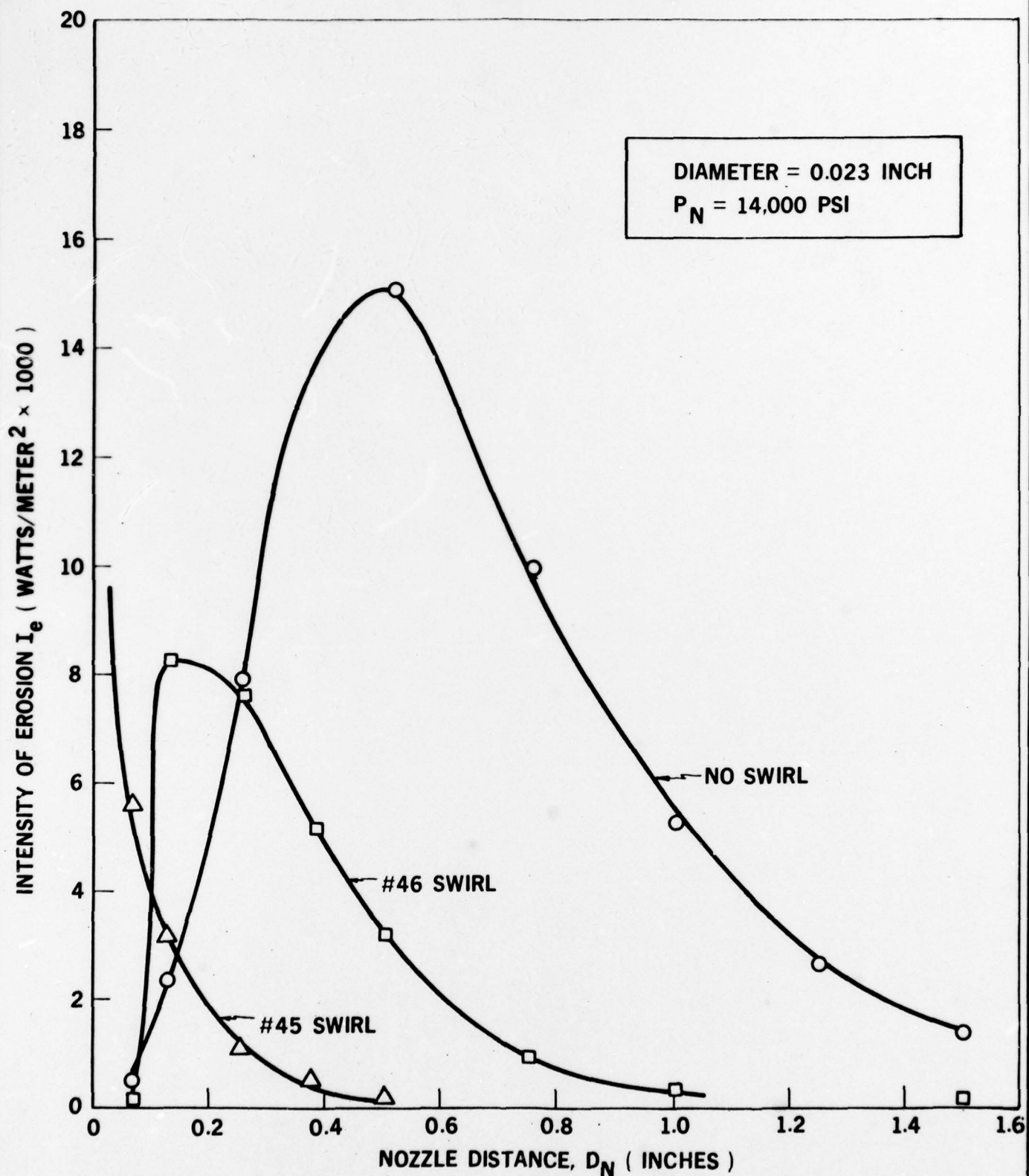


FIGURE 16 INTENSITY OF EROSION AS A FUNCTION OF NOZZLE DISTANCE FOR THREE CONFIGURATIONS OF THE 0.023 INCH DIAMETER NOZZLE, OPERATING PRESSURE = 14,000 PSI



DAEDALEAN ASSOCIATES, Inc.

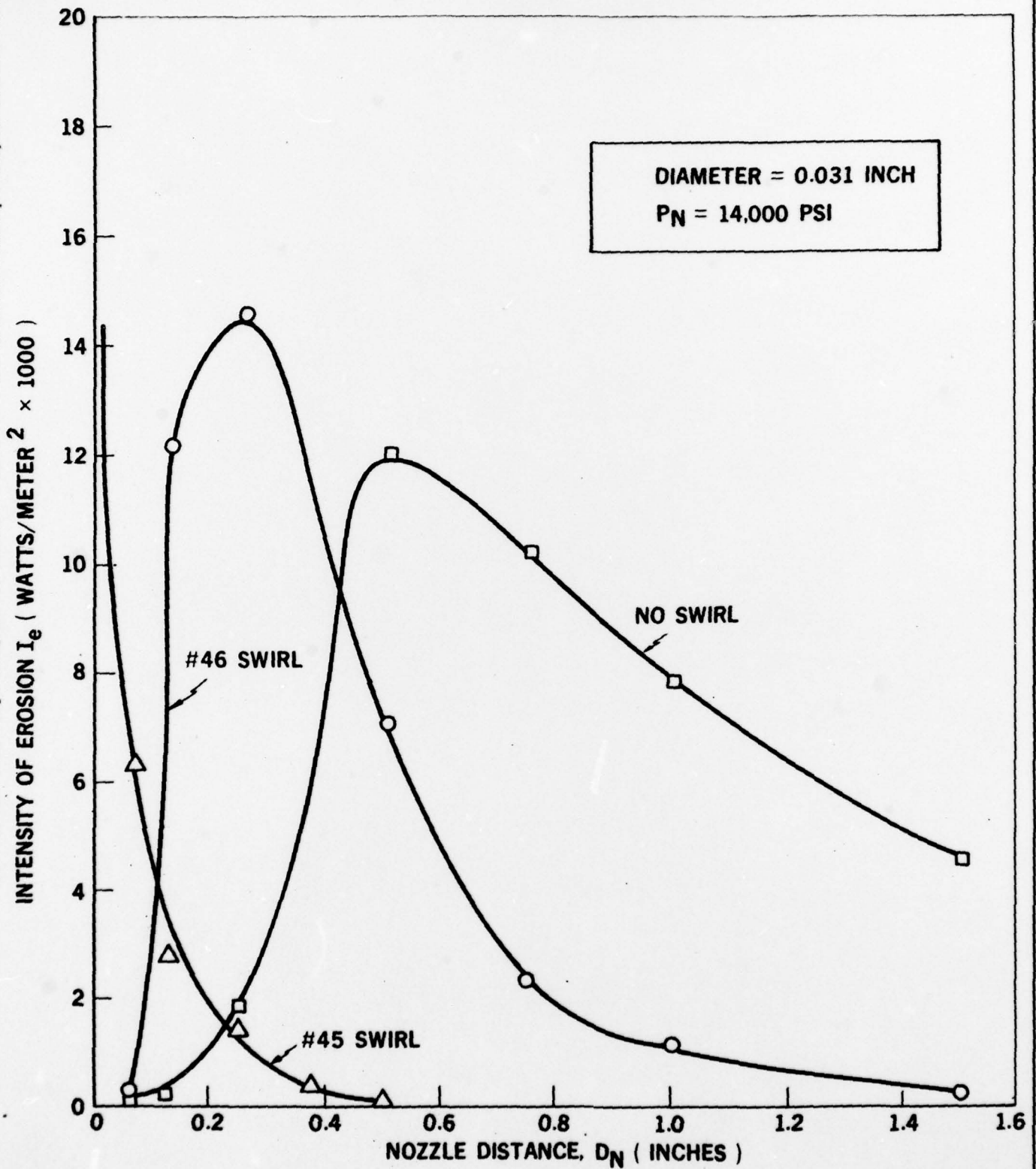


FIGURE 17 INTENSITY OF EROSION AS A FUNCTION OF NOZZLE DISTANCE FOR THREE CONFIGURATIONS OF THE 0.031 INCH DIAMETER NOZZLE, OPERATING PRESSURE = 14,000 PSI

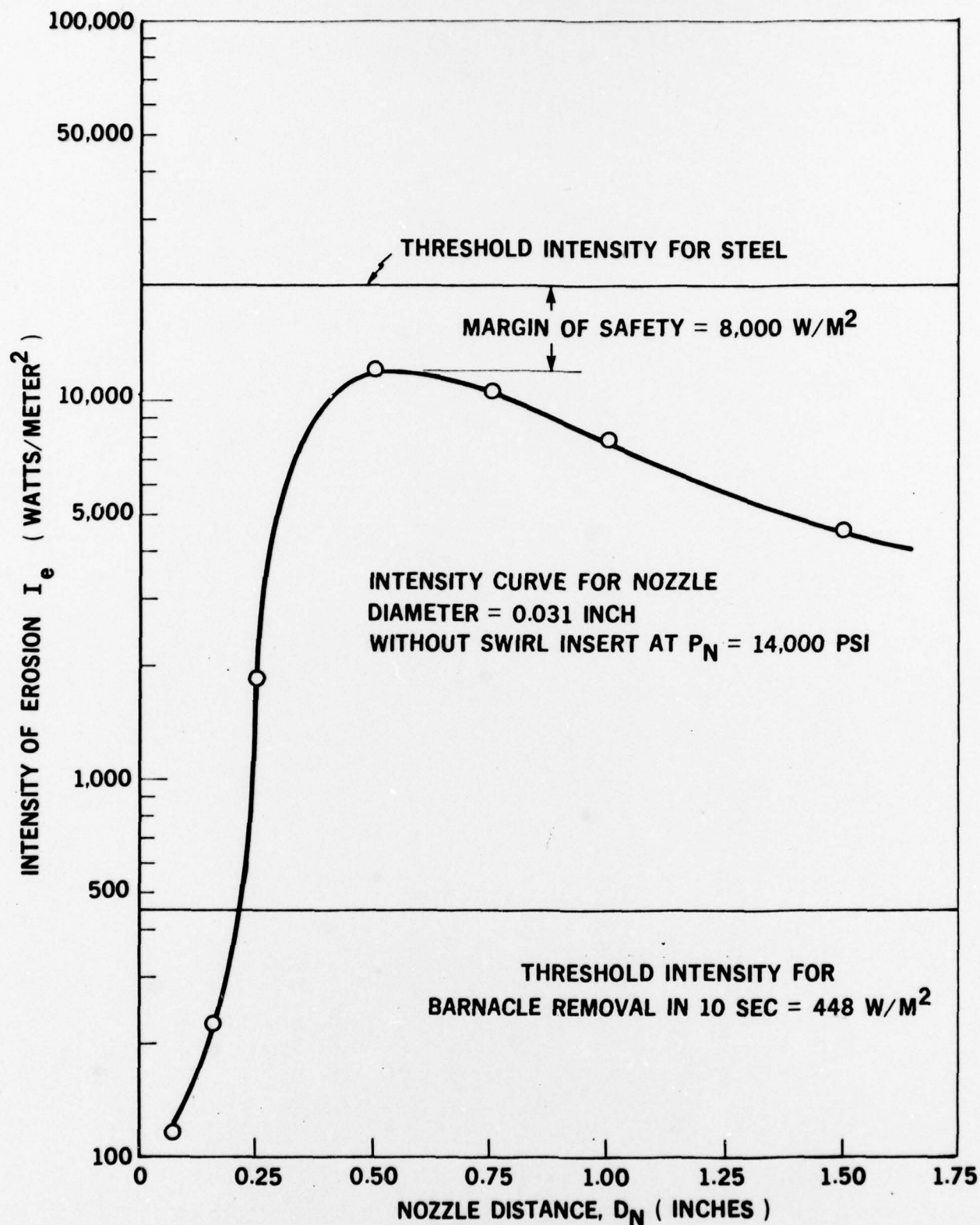


FIGURE 18 THRESHOLD INTENSITY FOR BARNACLE REMOVAL FROM PLATFORM STRUCTURE

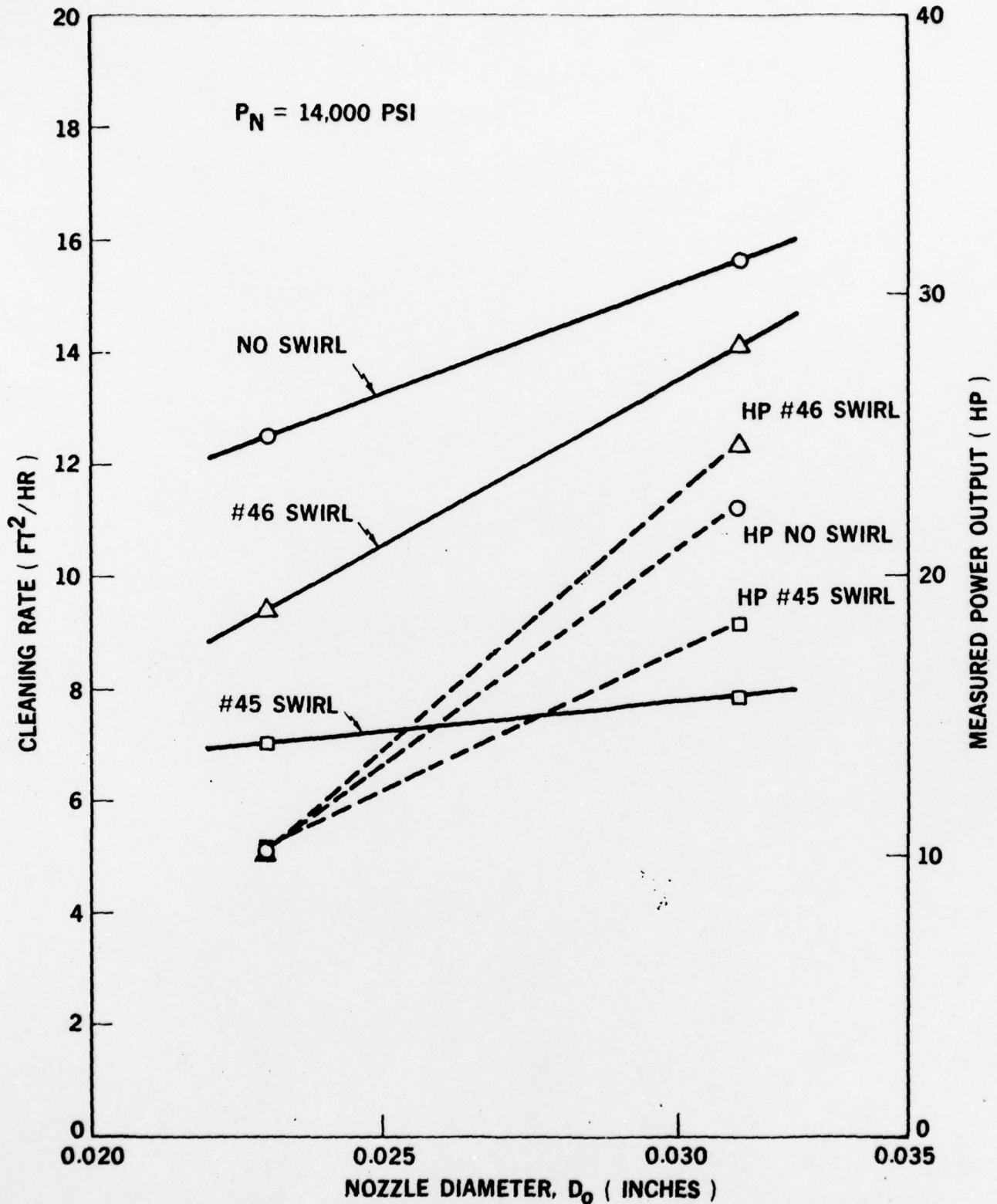


FIGURE 19 MEASURED POWER OUTPUT AND CLEANING RATE AS A FUNCTION OF NOZZLE DIAMETER USING SINGLE ORIFICE NOZZLES WITH AND WITHOUT SWIRLS

DAEDALEAN ASSOCIATES, Inc.



FIGURE 20 TEST PANEL FROM WHICH THE EPOXY VINYL COATING AND FOULING WAS REMOVED  
FROM ONE HALF THE AREA AT A CLEANING RATE OF 16 FT<sup>2</sup>/HR



DAEDALEAN ASSOCIATES, Incorporated

APPENDIX A

DESCRIPTION OF CAVITATION PHENOMENA

In most engineering contexts, cavitation is defined as the process of formation of the vapor phase of a liquid when it is subjected to reduced pressures at constant ambient temperature. In general, a liquid is said to cavitate when vapor bubbles are observed to form and grow as a consequence of pressure reduction. When the phase transition is a result of pressure change by hydrodynamic means, a two-phase flow composed of a liquid and its vapor is called a cavitating flow. While these definitions imply a distinction between phase transitions associated with reduction of pressure, on the one hand, and addition of heat (i.e. boiling), on the other, heat-transfer effects may play an important role in many cases of cavitating liquids. Such effects are especially of importance in liquids near their boiling points. From a purely physical-chemical point of view, of course, no distinction need be made between boiling and cavitation, at least insofar as the question of inception is concerned, and many of the basic physical ideas regarding inception, vapor mass transfer, and condensation apply equally.

As cavitation just begins, tiny vapor bubbles form in rapid succession at the point of lowest pressure and are carried downstream by the flow into a zone of higher pressure, where they immediately collapse as the vapor within them condenses. The process of formation and collapse is so nearly instantaneous

that with the naked eye only a continuous opaque blur can be distinguished. However, as each of the countless individual bubbles collapses, the resulting impact of opposing masses of liquid produces an extremely great local pressure which is transmitted radially outward with the speed of sound, followed by a negative pressure wave which may lead to one or more repetitions of the vaporization-condensation cycle. Boundary materials in the immediate vicinity are, therefore, subject to rapidly repeated stress reversals and may eventually fail through fatigue, the first sign of which is cavitation erosion.

An increase in the velocity of flow beyond that required for incipient cavitation can produce no further reduction in pressure at the point of cavitation, but merely an elongation of the zone over which the vapor limit prevails. At the same time the size of the vapor bubbles increases, until at advanced stages a more or less stable vapor pocket is formed, which is very similar in shape to the zone of separation next to an unstreamlined boundary. Since the formation of such a pocket must result in a change of the surrounding flow pattern, it is to be expected that the pressure distribution will change accordingly, the pressure necessarily remaining at its vapor limit throughout the length of the cavitation pocket.

For the purposes of this program, the phenomena of cavitation is the formation, growth and collapse of vapor cavities formed from nuclei. Water will provide the continuous medium

for the cavitation process. As the vapor cavities form in the vicinity of the cavity envelope, the fouling is removed from the surface (Figure A-1). Figure A-2 is a photographic representation of the cavity envelope during which the cavitation process is developed. The process is initiated from a nuclei which forms, grows to critical size, and collapses. Recent experiments conducted at the DAEDALEAN facilities have determined the feasibility of this process as a method of effectively cleaning marine growth from ship hulls.



CAVITATION INCEPTION PARAMETER

A useful index for the cavitation phenomenon is formulated by introducing for the symbol  $P$  in the pressure parameter its minimum value  $P_v$ , the result being called the cavitation number:

$$\sigma = \frac{P_o - P_v}{\frac{1}{2} \rho V_o^2} \quad [1]$$

where:  $P_o$  = free stream pressure  
 $P_v$  = vapor pressure of liquid  
 $V_o$  = free stream velocity  
 $\rho$  = density of liquid

So long as  $\sigma$  has an appreciably greater numerical value than the minimum ordinate on the dimensionless pressure-distribution curve for a body of given form, the occurrence of cavitation is not to be expected at any point on the boundary. Once  $\sigma$  becomes approximately equal in absolute magnitude to the minimum ordinate, on the other hand, conditions of incipient cavitation should prevail, and at values of  $\sigma$  below this critical limit  $\sigma_i$  a marked effect upon the pressure distribution is to be expected.

In the case of body forms which result in separation, it is to be noted that cavitation will generally begin within the fine-scale eddies formed at the separation surface long

before the boundary pressure attains its vapor limit. As a result, it is then not possible to predict the magnitude of  $\sigma_i$  either by analytical means or by actual measurement of the pressure distribution in flow without cavitation. On the other hand, not only are boundary forms which properly guide the flow most subject to analytical determination, but they are also those least subject to cavitation. The process of streamlining, in other words, simultaneously lowers the magnitude of  $\sigma_i$  (i.e., the tendency toward cavitation) and makes it more accurately predictable by analytical means.

The cavitation inception parameter is to be experimentally determined in order to evaluate the optimum operating parameters and the efficiency of cleaning by the cavitating jet technique.

CAVITATING JET CLEANING TECHNIQUE

Cavitation cleaning is caused by the collapse of bubbles at or near the solid boundaries guiding high speed flow. Since the early cavitation experiences were encountered on ship propellers in a highly corrosive medium (seawater), there were some controversies as to whether the mechanism was corrosion or mechanical removal. However, it is now generally accepted that the high pressures caused by the collapse of bubbles produce mechanical removal of material. During the process of cavitation a certain volume of material is removed from the surface as a result of the work done by the bubble collapse forces. The energy absorbed by the material is given by:

$$E = \Delta V \cdot S \quad [2]$$

where:  $E$  = energy absorbed by the material removed

$\Delta V$  = volume of material removed

$S$  = scale strength which represents the energy absorbing capacity of the material per unit volume under the action of the forces.

The intensity of cavitation is then defined as the power absorbed by the material per unit area and given by:

$$I = \frac{\Delta V \cdot S}{A \cdot \Delta t} \quad [3]$$

or

$$I = \frac{\Delta y}{\Delta t} (S) \quad [4]$$

where:  $A$  - area of cleaning

$\Delta y$  = mean depth of scale =  $\frac{\Delta V}{A}$

$\Delta t$  = exposure time

This is the output intensity of cleaning as seen by the material; similarly one can derive an expression for the bubble collapse intensity which is the input to the cleaning process.

$$\left( \frac{\Delta y}{\Delta t} \right) \cdot (S) \propto (P_i) \cdot (R) \cdot (n) \quad [5]$$

where:  $P_i$  = impact pressure

$R$  = size of the bubble or jet

$n$  = number of impacts per unit time

These ideas have been incorporated into a master chart for cavitation cleaning as shown in Figure A-3. In this chart, the intensity of erosion is plotted against the rate of mean depth of erosion for various materials ranging from soft lead to very highly resistant stellites. The range of intensities typical of practical machines varies from  $10^3$ - $10^4$  in.-lb/year-in.<sup>2</sup>. (The screening tests such as the vibratory test and



rotating disk test operate at intensity levels on the order of  $10^5$  in.-lb/year-in.<sup>2</sup> (1 watt/m<sup>2</sup>). The depth of erosion is generally in the range of a fraction of an inch per year. Chemical corrosion rates on steels are in the range of  $10^{-3}$ - $10^{-2}$  in. per year (ipy). Erosion rates on the order of 1 ipy represent serious erosion which may warrant operational limitation or redesign.

The level of threshold intensities for various metals are on the order of  $10^{-1}$  w/m<sup>2</sup> at the most. Elimination of cavitation by the substitution of one metal for another is possible only up to this level of intensity. For this reason, the usefulness of cathodic protection also seems to be limited at this level. If one is prepared to tolerate some erosion and periodic maintenance, then the materials selected coupled with cathodic protection can possibly extend the allowable intensity levels up to 1 w/m<sup>2</sup>. However, if the intensity levels are higher than these values, then the foregoing protection methods may not work. In such cases, hydrodynamic redesign, air injection, and specifying limits for operation are the alternate remedial possibilities.

Another tool for the benefit of designers and operators is a multipurpose nomogram as shown in Figure A-4. It provides a visual idea of the range of intensities encountered in actual practice within the range of the depth of cavitation material used and time of operation. It also provides a

quick and easy method of estimating the intensity of cavitation for a given field installation. Lastly, the selection of better materials, if available, is easily made.

From such tools as the master chart and the nomogram, it is possible to estimate the intensity of cavitation required to remove the marine growth and fouling most efficiently at the optimum rate of cleaning without damage to the platform structure. The intensity of cleaning can be adjusted to the required level.

DAEDALEAN ASSOCIATES, Inc.

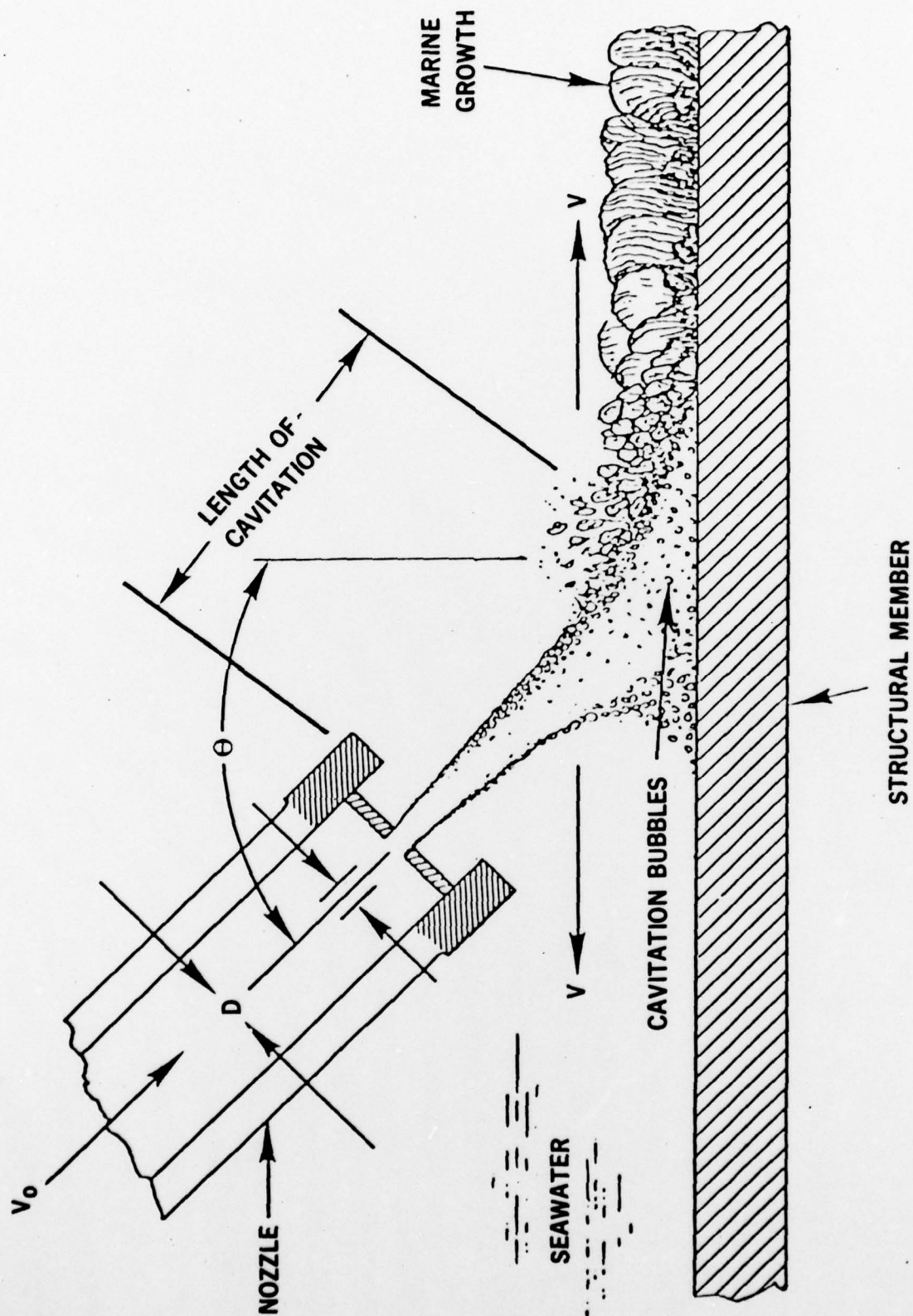


FIGURE A-1 PRINCIPLE OF CONTROLLED CAVITATION CLEANING TECHNIQUE AS APPLIED TO REMOVAL OF MARINE GROWTH AND FOULING FROM OFFSHORE PLATFORM STRUCTURAL MEMBER

DAEDALEAN ASSOCIATES, Inc.

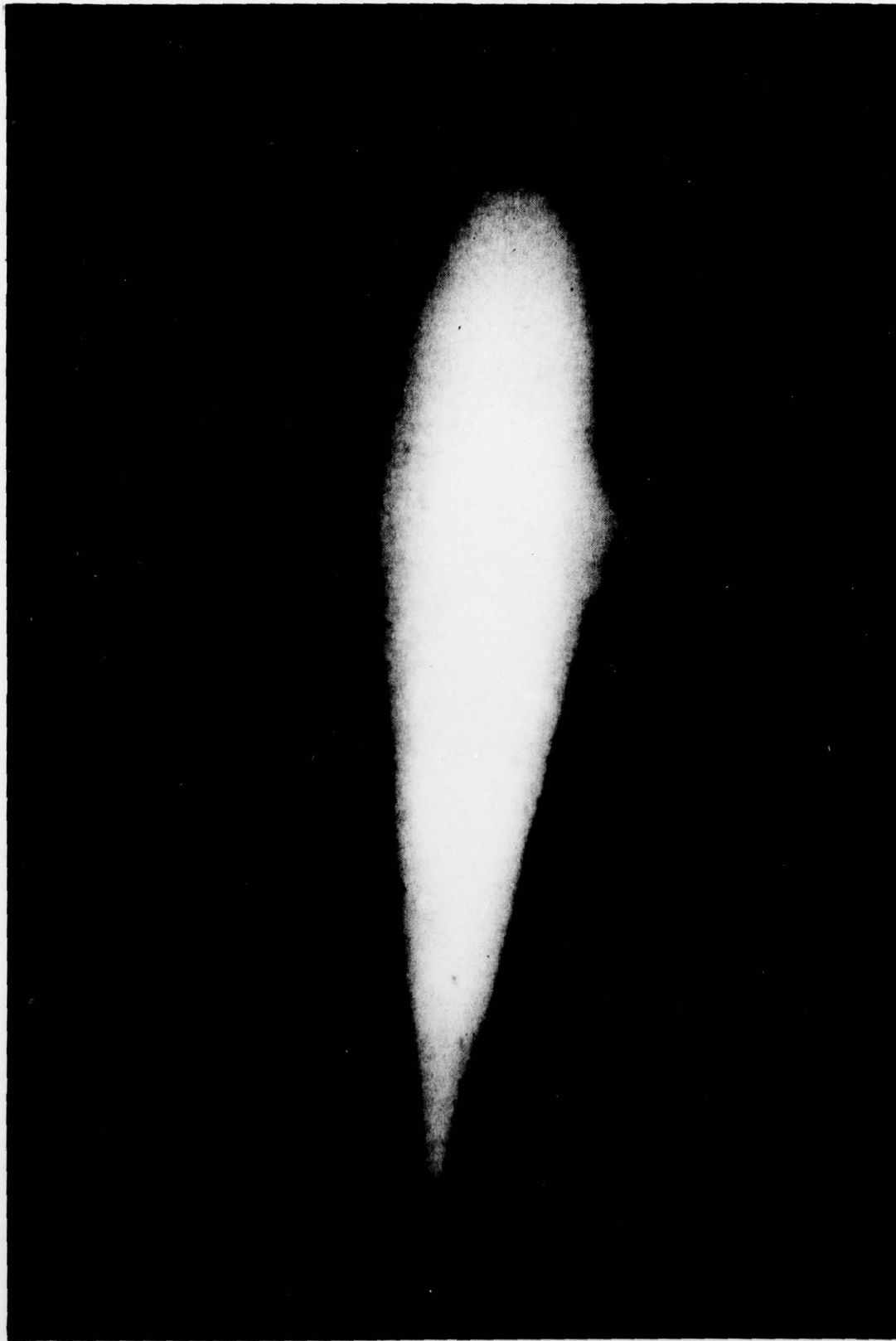


FIGURE A-2 PHOTOGRAPHIC REPRESENTATION OF THE CAVITATING ENVELOPE DURING WHICH TIME THE BUBBLES FORM A NUCLEI, GROW TO CRITICAL SIZE AND COLLAPSE IN THE CONTINUOUS CAVITATION PROCESS



DAEDALEAN ASSOCIATES, Inc.

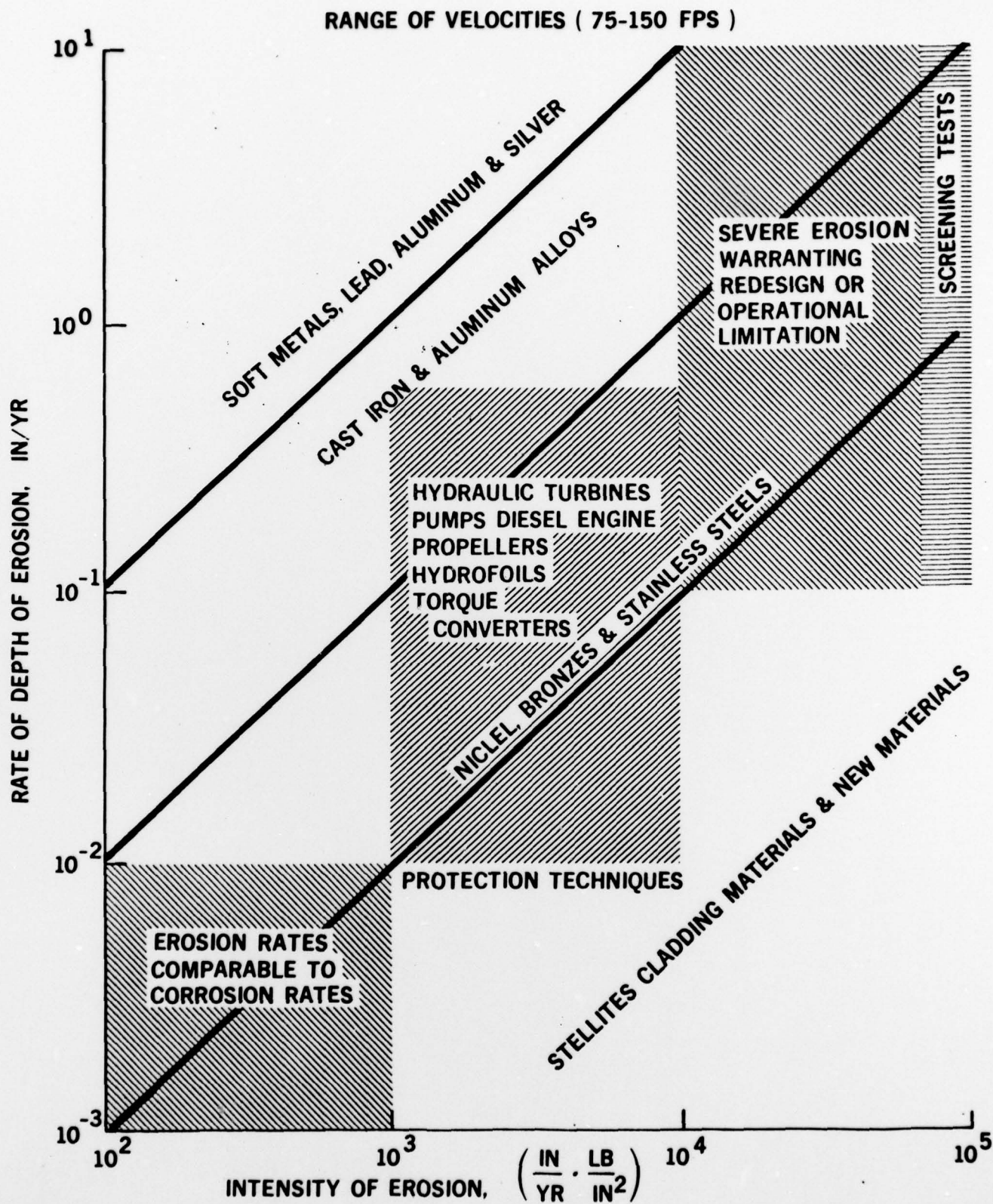


FIGURE A-3 MASTER CHART FOR CAVITATION EROSION

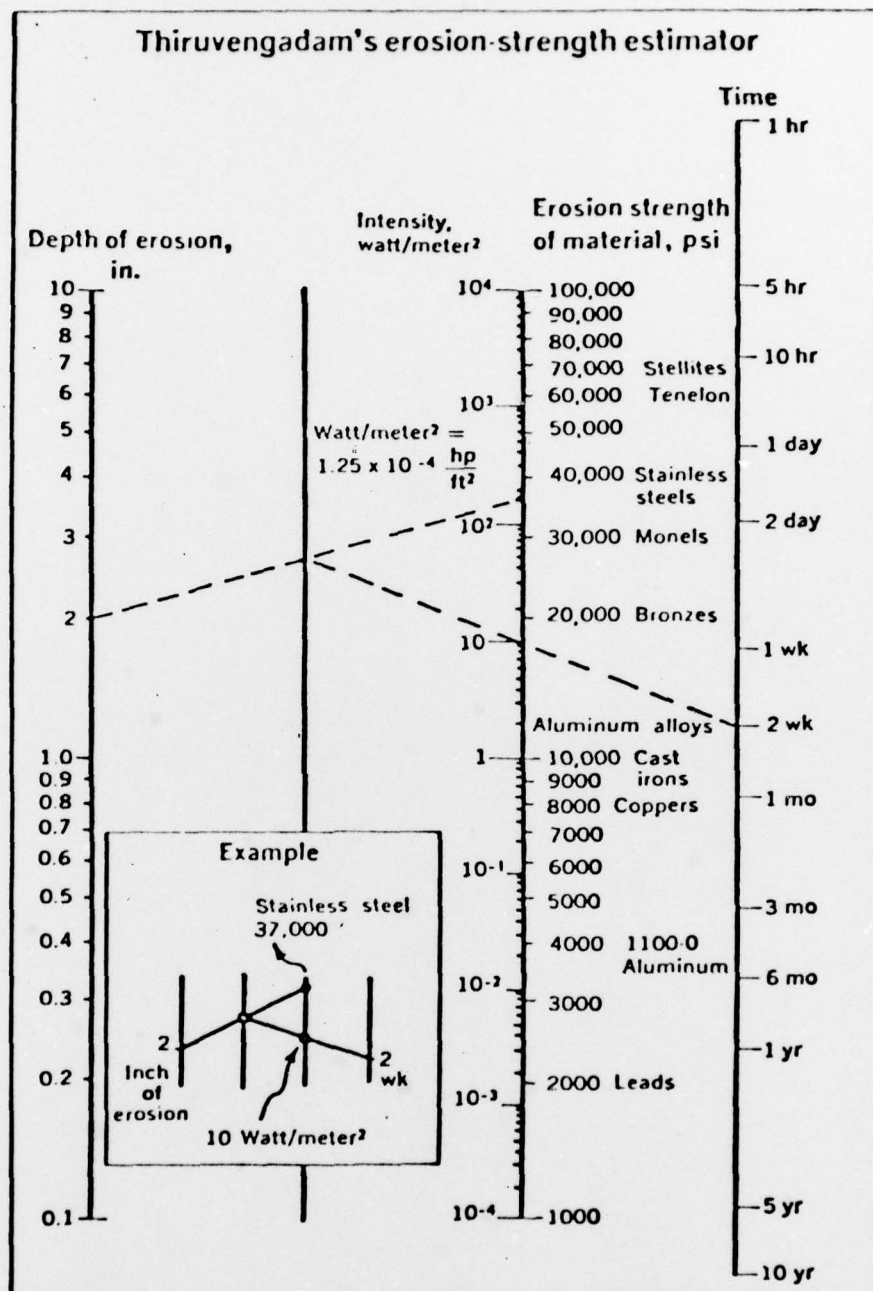


FIGURE A-4 EROSION INTENSITY ESTIMATOR